

Measuring similarity- and complementarity-driven relations in networks

Szymon Talaga^{1*}

Andrzej Nowak^{2,3}

¹Robert Zajonc Institute for Social Studies, University of Warsaw,
Stawki 5/7, 00-183 Warsaw, Poland.

²Faculty of Psychology, University of Warsaw,
Stawki 5/7, 00-183 Warsaw, Poland.

³Department of Psychology, Florida Atlantic University,
777 Glades Rd, Boca Raton, FL 33431, USA.

*Corresponding author; E-mail: stalaga@uw.edu.pl

Abstract

Structure of real-world networks is often shaped by similarity, meaning that two nodes are more likely to be linked if they are alike. However, some processes such as division of labor are driven rather by complementarity or differences and synergies. While it is well-known that similarity is associated with high abundance of triangles (3-cycles), there is no such result for complementarity. We argue that quadrangles (4-cycles) are the characteristic motif for complementarity-driven relations. Starting from very general geometric arguments we introduce two families of coefficients measuring the extent to which relations are shaped by similarity or complementarity. We study their main properties and show, through several case studies, that they can be used to distinguish between different kinds of social relations or networks from different domains as well as detect groups of similar or complementary nodes. Our results suggest that both similarity and complementarity are important processes shaping real-world networks.

1. Introduction

Complex systems in many fields of science and engineering ranging from physics to biology to sociology can often be effectively represented as networks, that is, in terms of sets of discrete entities (nodes or vertices) and relations between them (edges or links). The structure of networks is commonly indicative of functional properties of systems they represent as well as mechanisms or processes that created them. For instance, there is a large and growing body of evidence showing that the abundance of triangles (cycles traversing 3 nodes) is a structural signature of relations driven by similarity between nodes in some (possibly latent) metric space [8, 9, 11, 28, 47]. More generally, it is one of the important insights of the network science that statistical overrepresentation of particular motifs (small subgraphs) is very often informative of the underlying generating processes and/or functional properties of the system [35].

The importance of similarity-driven relations and their impact on structure of social networks has been recognized in sociology for a long time as they are linked to homophily, a tendency to connect to others who are similar to us with respect to some salient social, cultural or biological attributes [34]. Geometry induced by similarity has been also used for modeling of networks from other domains, including protein-protein interaction and brain networks [3, 22] as well as the Internet [10]. In such geometric models it is typically assumed that nodes are embedded in some feature space (observed or latent) and the probability of observing a link between two nodes is a monotonic function of distance between them. In particular, most of currently studied models are similarity-driven and assume that the link probability function is decreasing with respect to distance. This family is often referred to as Random Geometric Graph (RGG) [9, 15, 47] models.

The core insight provided by RGG models is that high abundance of triangles is indicative of relations driven by similarity (short distance in a feature space) implying that a network has either implicitly or explicitly geometric structure [28]. In other words, triangles are the characteristic motif for similarity-driven relations. This link between (latent) geometry and similarity is already a well-established fact within the general network science literature.

However, while important, similarity cannot be the only relational principle organizing structure of networks. For instance, some relations such as cooperation, business interactions or particular types of protein-protein binding may be better explained by complementarity or synergy between diverse features of the involved agents [14, 30, 53]. Hence, it is natural to ask whether there are motifs characteristic for complementarity-driven networks, in the same way as triangles are characteristic for similarity? And whether there is some latent geometric principle that would explain it? This problem of structural signatures of complementarity and their geometric interpretation has attracted much less attention than similarity, but it is no less fundamental and needs to be addressed.

The main goal of this paper is twofold. First we generalize some classical and some more recent results and define a geometrically motivated graph-theoretical measures of similarity-driven relations applicable not only to nodes but also to individual edges as well as entire networks. The focus is not on defining an explicit geometric generative model, but rather on deriving purely combinatorial coefficients (akin to the well-known local clustering [52]) from a very general geometric argument. Secondly, we consider a simple geometric model of complementarity-driven relations and use it to argue that quadrangles (4-cycles) are their characteristic motif. Then, we define corresponding complementarity coefficients following an analogous logic as in the case of similarity.

We will call the proposed measures *structural coefficients* because they will not be defined with respect to node attributes, latent or observed, but to how different nodes are embedded in the network and connected to their 1- and 2-hop neighbors. Moreover, we will show that they are closely linked to the notion of structural equivalence [36, 51].

The rest of the paper is structured as follows. First, we discuss local clustering and closure coefficients measuring the abundance of triangles and combine them in a new structural measure of similarity applicable at the level of edges, nodes and entire graphs. Then, we introduce the motivating geometric model of complementarity and use it to deduce the characteristic network motif for complementarity-driven relations (quadrangle). Next, we define quadrangle-based clustering and closure coefficients and combine them in a general structural measure of complementarity. We also discuss a natural connection between complementarity and bipartiteness. Then, we introduce a notion of weak complementarity which relaxes some of the assumptions and generalize all proposed coefficients to the case of weighted networks. Next, we study the behavior of the proposed measures in some of the most fundamental random graph models and apply structural similarity and com-

plementarity coefficients to a range of empirical datasets and research questions. For instance, we show that they can be related to meaningful domain-specific phenomena or used for discriminating between different kinds of relations as well as detection of groups of structurally similar and/or complementary nodes. We end by concluding remarks and a discussion of promising connections to other results.

Last but not least, all methods introduced in this paper are implemented in a Python package called `pathcensus` (see Sec. 4.2). It will be distributed through *Python Package Index* upon publication.

Datasets used and technical details including efficient methods for computing the proposed structural coefficients are discussed in Sec. 4 (Materials and methods) as well as Supplementary Materials (SM). In particular, we discuss algorithms for counting triples/quadruples and triangles/quadrangles. Summary of the notation is presented in Tab. 1.

1.1. Notation & technical remarks

In this paper we consider simple undirected graphs $G = (V, E)$. We use $n = |V|$ and $m = |E|$ to denote numbers of nodes and edges in G respectively. Elements of the adjacency matrix of a graph G will be denoted by a_{ij} and assumed to be equal to 1 if the edge (i, j) exists and 0 otherwise. For any node $i \in V$ we denote its degree by d_i and its k -hop neighborhood by $\mathcal{N}_k(i)$, in particular 1-hop neighborhood will be denoted by $\mathcal{N}_1(i)$. Moreover, we will use $n_{ij} = |\mathcal{N}_1(i) \cap \mathcal{N}_1(j)|$ to denote the number of shared neighbors between nodes i and j . Averaged quantities will be denoted by diamond brackets. For instance, $\langle d_i \rangle$ will denote average node degree.

All measures will be first introduced for the unweighted case but later also generalized to weighted networks. Therefore, when needed, the weight of an edge (i, j) will be denoted by w_{ij} . Moreover, for reasons that will soon become clear, we will use a somewhat non-standard notation and denote the strength of a node i (sum of its weights) by w_i instead of the commonly used s_i .

2. Results

2.1. Similarity-driven relations

It is arguably natural to think about similarity in terms of distance between different objects in a feature space. Hence, the motivating geometric model for similarity-driven relations posits that nodes are positioned in some metric space and the probability of observing a link between them is a decreasing function of the corresponding distance. Such a generic model can be seen as an instance of the class of Random Geometric Graphs (RGGs) [9, 47]. The crux is that this very general formulation is enough to guarantee a high abundance of triangles (3-cycles), provided that the link probability function decreases with respect to distance at a high enough rate [28]. In other words, triangles are the characteristic network motif for similarity-driven relations (see Fig. 1A).

In this light, a natural starting point for our endeavor is *local clustering coefficient* [52], of which value for node i will be denoted by s_i^W . It is a classical network measure of how dense the 1-hop neighborhood of i is and it is defined as:

$$s_i^W = \frac{2T_i}{t_i^W} \quad (1)$$

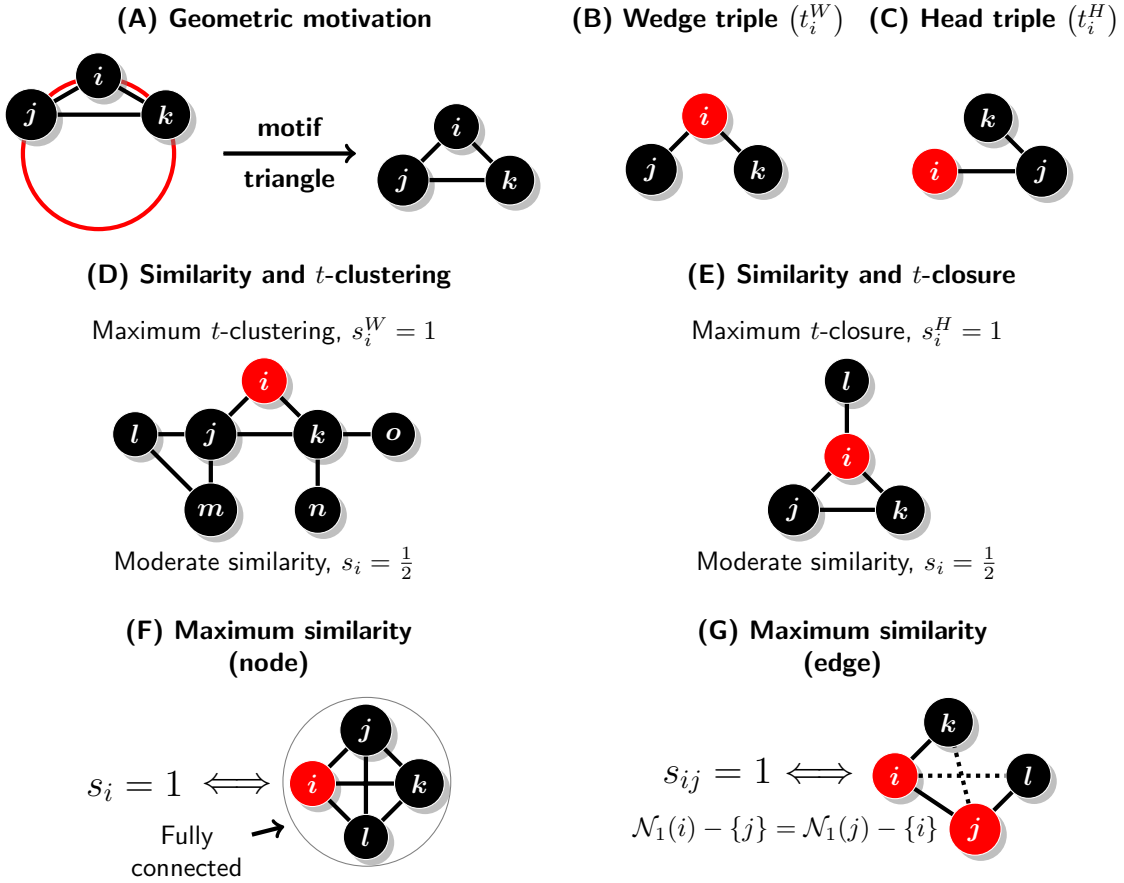


Figure 1. Geometric motivation and overview of main properties of structural similarity coefficients. (A) Metric structure induced by similarity leads to the abundance of triangles making them its characteristic motif. (B and C) Wedge and head triples. (D) Local clustering can be maximized even when neighbors of the focal node are very differently embedded within the network, while s_i correctly recognizes this fact. (E) Local closure can be maximized even for nodes with sparse 1-hop neighborhoods if they are star-like as neighbors with degree one do not generate any head triples. On the other hand, s_i is sensitive to this deviation from the similarity-driven pattern of connections. (F and G) Necessary and sufficient conditions for maximum structural similarity coefficient at the levels of nodes and edges.

where T_i is the number of triangles including i and t_i^W is the number of wedge triples centered at i or 2-paths with i in the middle (Fig. 1B). Crucially, $s_i^W \in [0, 1]$ and is equal to 1 if and only if $\mathcal{N}_1(i)$ forms a fully connected network. In sociological terms it measures the extent to which *my friends are friends with each other*. Note, however, that this is only one side of the triadic closure process [27] as it corresponds to the closing of the loop between friends of the focal node i . The other part is about closing the loop between i and friends of its friends and local clustering coefficient does not capture it.

To address this issue a new *local closure coefficient* [54] has been proposed more recently:

$$s_i^H = \frac{2T_i}{t_i^H} \quad (2)$$

where t_i^H is the number of head triples originating from i , that is, 2-paths starting at i (Fig. 1C). It is also in the range of $[0, 1]$ and attains the maximum value if and only if no neighbor of i is adjacent to a node which is not already in $\mathcal{N}_1(i)$. In other words, when $s_i^H = 1$ a random walker starting at i will never leave $\mathcal{N}_1(i)$. Thus, local closure coefficient measures the extent to which *friends of my friends are my friends*, that is, it is a measure of triadic closure between the focal node i and neighbors of its neighbors. As a result it captures exactly that what local clustering is blind to. Since local clustering and closure coefficients are based on triples we will later refer to them as t -clustering and t -closure respectively.

The two coefficients complement each other so it is only natural to combine them in a single measure. We now propose such a measure which we will call *structural similarity coefficient*:

$$s_i = \frac{4T_i}{t_i^W + t_i^H} = \frac{t_i^W s_i^W + t_i^H s_i^H}{t_i^W + t_i^H} \quad (3)$$

Note that s_i is equal to the fraction of both wedge and head triples including i which can be closed to make a triangle. It is also equivalent to a weighted average of s_i^W and s_i^H , which implies that $\min(s_i^W, s_i^H) \leq s_i \leq \max(s_i^W, s_i^H)$. Moreover, since $s_i^W = 1$ if and only if $\mathcal{N}_1(i)$ is fully connected and $s_i^H = 1$ if there are no links leaving $\mathcal{N}_1(i)$ then it must be that $s_i = 1$ if and only if i belongs to a fully connected network (Fig. 1F), so in the limit as $s_i \rightarrow 1$ the coefficient becomes a global measure describing the structure of the entire component containing i . Note that it is a proper measure of the degree to which local neighborhood around i is driven by similarity as it attains the maximum value only when i and all nodes around it form a tightly knit community and are structurally redundant in the sense that the removal of any of the nodes does not affect the connectivity of the graph. Fig. 1 provides a summary of the motivation and main properties of s_i , including examples of when t -clustering and t -closure coefficients may be maximum while structural similarity is only moderate (Figs. 1D and 1E).

Another advantage of s_i is that it is defined for all nodes included in at least one 2-path, so, unlike t -clustering coefficient which is undefined for nodes with degree one [54], it is almost always defined. Moreover, in general under the configuration model [36, ch. 12] t -clustering often decreases with node degree on average (or at least does not increase) while t -closure increases [54]. Hence, since s_i is bounded between s_i^W and s_i^H it can vary in diverse, also non-monotonic, ways with respect to node degree. We elaborate on this more in Sec. 2.5.

2.1.1. Edge-wise similarity and structural equivalence

Structural similarity coefficient can also be defined for edges. In this case it is equal to the ratio of triangles including nodes i and j to the total number of 2-paths traversing the (i, j) edge (Fig. 1G). In other words, it is equivalent to the number of shared neighbors relative to the total number of neighbors of i and j , excluding i and j themselves:

$$s_{ij} = \frac{2T_{ij}}{t_{ij}^W + t_{ij}^H} = \frac{2n_{ij}}{d_i + d_j - 2} \quad (4)$$

where T_{ij} is the number of triangles including i and j , t_{ij}^W is the number of (k, i, j) and t_{ij}^H of (i, j, k) triples. Importantly, s_{ij} is symmetric since $T_{ij} = T_{ji}$ and $t_{ij}^W = t_{ji}^H$.

Note that s_{ij} is closely related to the Sørenson Index or normalized Hamming similarity [36, 43], $H_{ij} = 2n_{ij}/(d_i + d_j)$, and differs only in the -2 term in the denominator which accounts for the fact that i and j are known to be connected. Hamming distance/similarity is one of the common measures of structural equivalence [Sec. 7.12.3 in 36] which implies that the proposed node-wise similarity coefficient can be seen as a proxy for the extent to which i is structurally equivalent to its own neighbors. More concretely, since s_i can be expressed as a weighted average of s_{ij} 's for $j \in \mathcal{N}_1(i)$ we have that:

$$\min_j H_{ij} < s_i \leq \max_j \left(H_{ij} \frac{d_i + d_j}{d_i + d_j - 2} \right) \approx \max_j H_{ij} \quad (5)$$

In other words, local similarity coefficient of a node i is approximately bounded between minimum and maximum structural equivalence between i and any of its neighbors (see SM: S1 for the derivation). This justifies the interpretation of the proposed similarity coefficients in terms of *structural similarity*.

2.1.2. Global similarity coefficient

From the global perspective both local clustering and local closure lead to the same conclusion that the corresponding global measure of clustering/closure is just the fraction of triples that can be closed to make a triangle [54]. This implies that the same quantity is also the proper global measure of the extent to which relations are driven by similarity. In other words, the *global similarity coefficient* is equal to the standard global clustering coefficient and can be defined as:

$$s = \frac{3T}{\sum_i d_i(d_i - 1)} \quad (6)$$

where T is the total number of triangles and the denominator counts the number of triples.

Note that it is indeed a reasonable measure of similarity-driven relations as it is maximized only when a network is fully connected, so all nodes are structurally redundant and can be removed without affecting the overall connectivity.

2.2. Complementarity-driven relations

First let us consider an intuitive meaning of complementarity. We posit that two objects are complementary when their features are different but in a well-defined synergistic way. As we will see, this additional synergy constraint is crucial. However, before we discuss this further let us note that in the case of similarity an analogous constraint is built-in by design. It is so, because for any point there is always only one point minimizing the distance in the feature space (maximizing similarity) and it is the point itself. Hence, it is arguably natural to say that any object is most similar to itself. As a result, there is a well-defined notion of maximal similarity.

On the other hand, the case of difference is more complex. To make our argument more concrete, let the feature space be \mathbb{R}^k with $k \geq 1$. Now, it is easy to see that for any two points p and r at a distance $d(p, r)$ we can find a third point s such that $d(p, s) > d(p, r)$. In other words, for any point p there is no well-defined point at the maximum distance. As a result, complementarity cannot be defined in terms of difference without some additional constraints. Intuitively, complementarity

understood in terms of unconstrained difference inevitably leads to the result that for any object there is an infinite variety of more and more complementary (different) objects, which clearly does not map well on the common understanding of the notion of complementarity. Thus, we need a definition with the same property as in the case of similarity, that is, one yielding a sequence of ever smaller sets of more and more complementary elements converging to a single well-defined point in the limit of maximum complementarity.

Note that the above abstract argument can be related to known complementarity-driven systems in a rather straightforward manner. For instance, antibodies produced by immune systems are not complementary to antigens because they are just different in an arbitrary manner, but because they differ in a very specific way by having binding sites which are structural negatives of a particular antigen. Similar logic of complementarity can be seen in many different phenomena from the division of labor to man-made tools (e.g. a key and a lock).

Thus, we argue that complementarity should be defined in terms of distance maximization but with additional constraints ensuring that for any point in the feature space there is only one point at the maximum distance. This can be achieved in several different ways, but to keep things simple we will focus on one particularly natural and convenient solution.

We now specify the motivating geometric model of complementarity-driven relations with appropriate constraints. We consider nodes as placed on the surface of a k -dimensional (hyper)sphere with $k \geq 2$. In this setting for each point there is only a single point at the maximum distance and the maximum distance is the same for all points. Now, if nodes connect preferentially to others who are far away, we obtain a model analogous to the similarity but now the connections of a node are not concentrated in its vicinity but instead on the other side of the space. From this it follows that any two connected nodes i and j will not share a lot of neighbors, so triangles will be very rare, but instead the 1-hop neighborhood of i should be approximately equal to the 2-hop neighborhood of j and *vice versa*, that is, $\mathcal{N}_1(i) \approx \mathcal{N}_2(j)$ and $\mathcal{N}_2(i) \approx \mathcal{N}_1(j)$. And such a spatial structure must inevitably lead to the abundance of quadrangles and in general locally dense bipartite-like subgraphs (Fig. 2A).

Note that the choice of a (hyper)sphere surface is far from arbitrary as it is a specific instance in the broader class of compact homogeneous and isotropic manifolds, for which it has been shown that it is a proper choice for a latent geometry capable of reproducing jointly sparsity with high clustering, small-world effect and arbitrary degree distributions in similarity-driven networks [9]. In other words, in this setting latent geometry can explain some of the most fundamental structural properties of real-world networks [47]. Thus, we argue, it is also a natural first choice for representing relations driven by complementarity, especially that thanks to its structure it seems particularly well-suited for this task (but see Ref. [26] for an alternative approach).

One more remark is needed at this point. Depending on the context different authors may refer to slightly different objects when using the term *quadrangle*. More concretely, a quadrangle may contain up to two chords or diagonal links between its vertices. For now, we will consider only quadrangles without any chords which we will call *strong quadrangles*. This choice follows, of course, from the proposed geometric model and the fact that only strong quadrangles are characteristic for locally dense bipartite graphs. However, in Sec. 2.3 we will generalize our approach to weaker notions of quadrangles allowing for the presence of chordal edges.

Now we can start defining coefficients measuring complementarity-driven relations. As previously, we begin with a local clustering coefficient which we will call q -clustering. It is defined

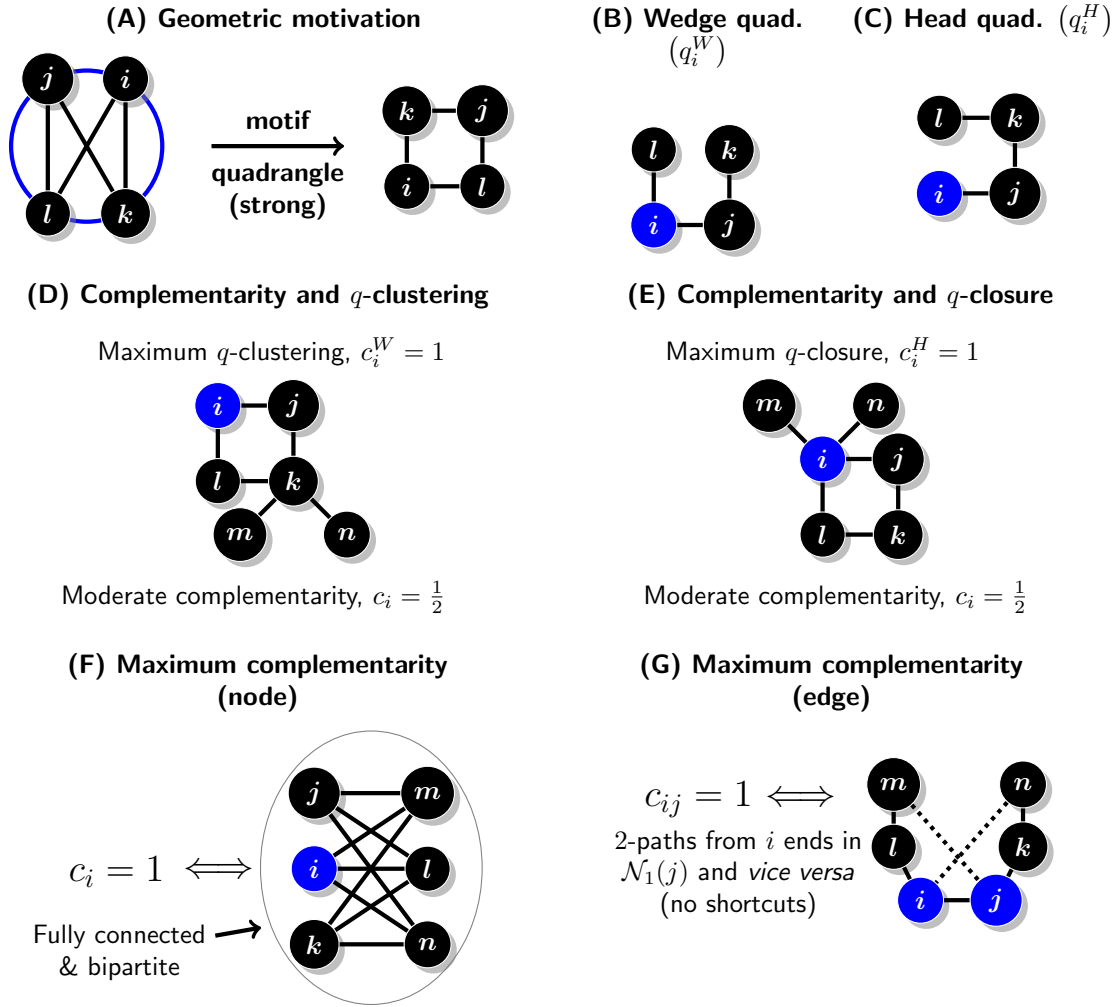


Figure 2. Geometric motivation and overview of main properties of structural complementarity coefficient. (A) On the surface of a (hyper)sphere for each point there is only a single other point at the maximum distance, so complementarity based on distance maximization must lead to the abundance of (strong or chordless) quadrangles and locally dense bipartite-like structures. (B and C) Wedge and head quadruples. (D) Local q -clustering can be maximized even when some 2-hop neighbors (node k on the figure) of the focal node connect to nodes which are not in $\mathcal{N}_1(i)$, while the complementarity coefficient correctly identifies this structure. (E) Local q -closure can be maximized even for nodes with sparse 1-hop neighborhoods if they are star-like as neighbors with degree one do not generate any head quadruples. (F and G) Necessary and sufficient conditions for maximum structural complementarity coefficient at the levels of nodes and edges.

analogously, but this time in terms of quadrangles and wedge quadruples, that is, 3-paths with the focal node i at the second position (Fig. 2B):

$$c_i^W = \frac{2Q_i}{q_i^W} \quad (7)$$

where Q_i is the number of quadrangles with no chordal, or diagonal, edges including the focal node i and q_i^W is the number of wedge quadruples it belongs to. Note that we consider only quadruples with i at the second position, such as (l, i, j, k) but not (k, j, i, l) , in order to avoid double counting and make the number of wedge and head quadruples per quadrangle equal. Intuitively, it quantifies the extent to which the local environment of i is bipartite-like and its neighbors are structurally equivalent to each other.

Local q -closure coefficient is defined in the same way as the fraction of head quadruples originating from i (Fig. 2C) that can be closed to make a (strong) quadrangle:

$$c_i^H = \frac{2Q_i}{q_i^H} \quad (8)$$

where q_i^H is the number of head quadruples starting at i . Conceptually, it measures the extent to which the local environment of i is bipartite-like and i is structurally equivalent to its 2-hop neighbors.

We can now define *structural complementarity coefficient* as the fraction of quadruples including the focal node i which can be closed to make a (strong) quadrangle which, again, is equivalent to a weighted average of q -clustering and q -closure:

$$c_i = \frac{4Q_i}{q_i^W + q_i^H} = \frac{q_i^W c_i^W + q_i^H c_i^H}{q_i^W + q_i^H} \quad (9)$$

Note that again we have that $\min(c_i^W, c_i^H) \leq c_i \leq \max(c_i^W, c_i^H)$. Moreover, the interpretations of q -clustering and q -closure jointly imply that $c_i = 1$ if and only if the focal node i belongs to a fully connected bipartite network. Fig. 2 presents a summary of the most important terms and facts related to c_i .

Last but not least, notice that the geometric model underlying the definition of c_i indeed justifies the interpretation in terms of complementarity or synergy. Nodes are more likely to be connected when they are far away in the feature space, meaning that they have different properties which can be possibly combined in a synergistic manner. Crucially, the mesoscopic network structure that is implied by this model is also related to complementarity in a straightforward manner. Bipartite networks are representations of complementarity-driven systems *par excellence* as they consist of two types of nodes and allow only for connections between them. Hence, c_i , being a combined measure of local bipartiteness and density, is actually indicative of the degree to which the local environment of a node resembles such a complementarity-driven system. Note that the fact that c_i is constrained by the density of bipartite connections is crucial as tree-like networks are also locally bipartite-like (i.e. $\mathcal{N}_1(i)$ corresponds to the first type and $\{i\} \cup \mathcal{N}_2(i)$ to the second) but in a trivial way as connections between the two “types” of nodes are very sparse, indicating rather a random organization, or at least such a structure cannot be interpreted as compelling evidence of complementarity.

Note that the proposed measures of structural complementarity are based on strong, chordless quadrangles and therefore are different from alternatives such as those proposed in Ref. [23], where authors used a weak definition of quadrangles allowing for any number of chords. This is important as only strong quadrangles lead to definitions which can be interpreted strictly in terms of dense locally bipartite structures and this, as we argue, is crucial for measuring complementarity-driven relations.

Furthermore, when applied to purely bipartite networks quadrangle-based measures can be seen as variations of the bipartite clustering coefficient [55]. However, the crux is that our quadrangle-

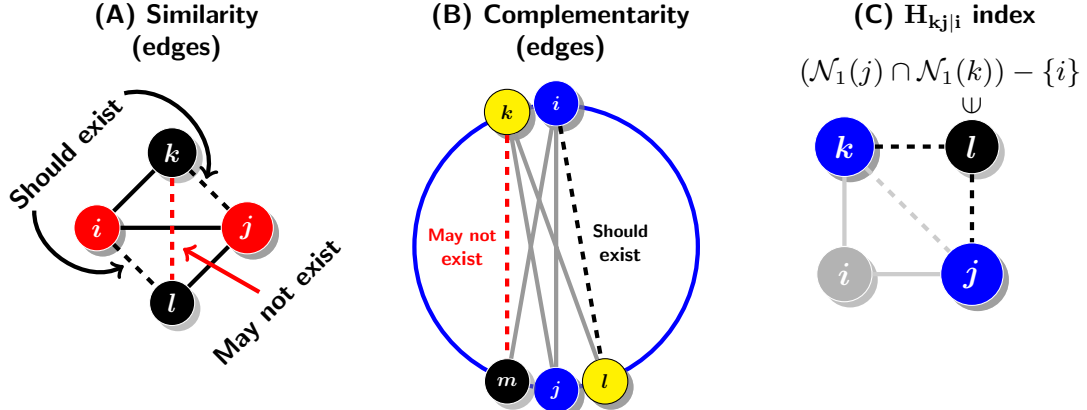


Figure 3. Interpretation of the edge-wise structural coefficients and Asymmetric Excess Sørenson Index. (A) If (i, j) edge is driven by similarity then any neighbor of either i or j (k and l on the figure) should be near i (or j) in the latent space making it likely that it links to the other member of the (i, j) pair too. On the other hand, k and l may still be quite far away so the link between them may not exist. (B) If (i, j) edge is driven by complementarity then any 2-hop neighbor of j (i), such as l (k) on the figure, should be a 1-hop neighbor of i (j). On the figure the quadruple (i, j, k, l) corresponds to such a situation. On the other hand, any pair of neighbors of i and j correspondingly may be located in the latent space close enough to each other as to make a tie between them unlikely (as it happens for nodes m and k on the figure). (C) Construction of the Asymmetric Excess Sørenson Index ($H_{kj|i}$) measuring how structurally equivalent is k with respect to j disregarding any direct links between i, j and k .

based complementarity coefficients can be also applied to unipartite networks in order to quantify jointly local bipartiteness and density, which together are indicative of complementarity-driven relations.

2.2.1. Edge-wise complementarity and structural equivalence

As for similarity, we can also measure local complementarity at the level of edges (Fig. 2G). The edge-wise coefficient is defined as:

$$c_{ij} = \frac{2Q_{ij}}{q_{ij}^W + q_{ij}^H} \quad (10)$$

where Q_{ij} is the number of (strong) quadrangles including nodes i and j , q_{ij}^W is the number of (j, i, k, l) and q_{ij}^H of (i, j, k, l) quadruples. Again, $Q_{ij} = Q_{ji}$ and $q_{ij}^W = q_{ji}^H$ so c_{ij} is symmetric.

This way c_{ij} can be seen as a joint measure of bipartiteness around an (i, j) edge and structural equivalence between i and 1-hop neighbors of j and *vice versa*. This way c_{ij} measures the extent to which $N_2(i) \approx N_1(j)$ and $N_1(i) \approx N_2(j)$ without requiring dense connections between the 1-hop and 2-hop neighborhoods of i and j . Note that this is analogous to edge-wise similarity which measures only the extent to which $N_1(i) \approx N_1(j)$ without considering the density of connections between the neighbors of i and j as this would be a higher-order property unrelated to whether an edge is driven by similarity or not (see Figs. 3A and 3B for details).

The formal connection between complementarity and structural equivalence is somewhat more complicated than in the case of similarity and we need to introduce one additional quantity. For a connected triple (k, i, j) we define *Asymmetric Excess Sørenson Index*:

$$H_{kj|i} = \frac{n_{jk} - 1}{d_k - 1 - a_{jk}} \quad (11)$$

which measures how structurally equivalent k is with respect to j while disregarding edges (i, k) , (i, j) and (j, k) . Note that the excess degree of k is used in the denominator as the (i, k) link needs to be ignored. Moreover, a_{jk} term accounts for the possible presence of the (j, k) link. Finally, 1 is subtracted from n_{jk} to account for the fact that i is a shared neighbor of j and k (see Fig. 3C).

It is possible to show that $c_{ij} \leq \max_{k,l}(H_{kj|i}, H_{li|j})$ for $k \in \mathcal{N}_1(i) - \{j\}$ and $l \in \mathcal{N}_1(j) - \{i\}$. Moreover, it can be shown that c_i is a weighted average c_{ij} 's. These two facts jointly imply that for $j \in \mathcal{N}_1(i)$, $k \in \mathcal{N}_1(i) - \{j\}$ and $l \in \mathcal{N}_1(j) - \{i\}$ the following inequality holds:

$$0 \leq c_i \leq \max_{j,k,l} (H_{kj|i}, H_{li|j}) \quad (12)$$

In other words, local complementarity around a node i is bounded from above by the maximum asymmetric structural equivalence between any pair of its neighbors or neighbors of its neighbors and itself. Crucially, this justifies the interpretation in terms of *structural complementarity*. See SM: S2 for the derivation and other details.

2.2.2. Global complementarity coefficient

From the global perspective of an entire network there is of course no difference between wedge and head quadruples. Hence, the global coefficient can be defined simply as:

$$c = \frac{4Q}{\sum_{i,j} (d_i - 1)(d_j - 1) - n_{ij}} \quad (13)$$

where $(i, j) \in E$ and Q is the total number of quadrangles with no chords. The denominator counts the total number of quadruples.

Note that $c = 1$ if and only if the graph as such is fully connected and bipartite. This agrees with the intuition as this is exactly the structure one should expect in a system composed of two classes of elements in which each element in one class is perfectly complementary to each element of the other.

2.3. Weak complementarity

The complementarity coefficients as we defined them are based on a rather strict notion of strong, or chordless, quadrangles. Compared to triangles, these are higher-order motifs composed of 4, instead of 3, nodes and as such they can be distorted in several different ways. While a triple is either open or closed, quadruples can form quadrangles with 0, 1 or 2 chordal (diagonal) edges. Given that real-world networks are hardly ever measured without error or produced by a single generating mechanism, using the strict definition based on strong quadrangles may sometimes be too restrictive. To address this problem we define also measures of *weak complementarity*.

They are defined in the same way as (strong) complementarity coefficients but instead of using counts of strong quadrangles in the numerator they are based on counting weak quadrangles allowing

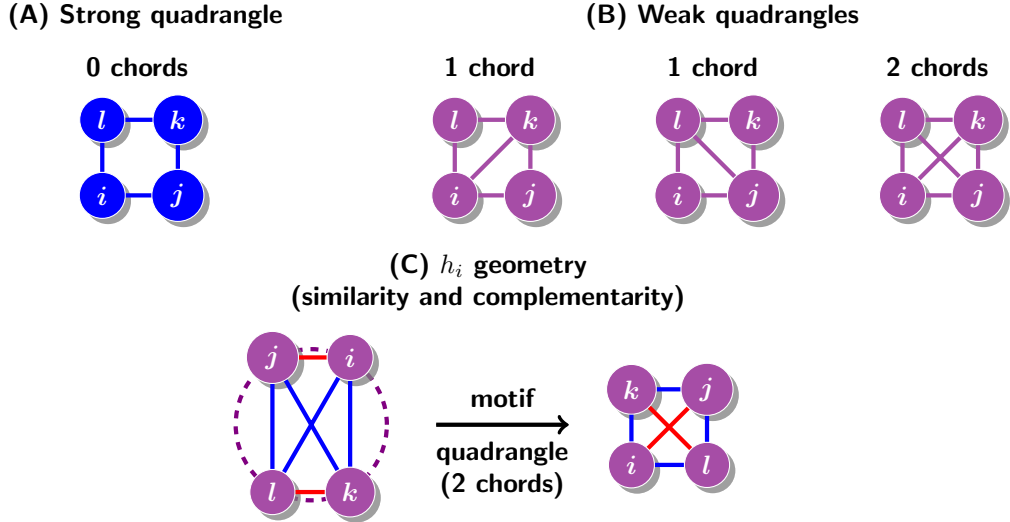


Figure 4. Overview of weak complementarity. Motifs corresponding to it are marked with violet color as its a mix of red (similarity) and blue (complementarity). **(A and B)** Possible types of quadrangles. **(C)** Geometric view of weak complementarity indicating that quadrangles with two chords are the characteristic motif for systems driven by both similarity and complementarity.

for the presence of chordal edges. Let us denote the count of quadrangles including a node i with exactly k chordal edges, for $k = 0, 1, 2$, by $Q_i^{(k)}$ (see Fig. 4A and 4B). Then, weak complementarity is defined as:

$$h_i = \frac{4 \left(Q_i^{(0)} + Q_i^{(1)} + Q_i^{(2)} \right)}{q_i^W + q_i^H} \quad (14)$$

where $Q_i^{(0)}$ is of course equal to Q_i . In what follows, we will use the two notations interchangeably.

The above is just a relatively straightforward generalization of Eq. (9). All other complementarity-related coefficients defined by Eqs. (7), (8), (10) and (13) are redefined in the same way, so we do not state them explicitly here for the sake of brevity. Instead, all the details regarding the definitions of structural coefficients are discussed in Sec. 4.1 and SM: S3.5.

While the strong complementarity coefficients measure the presence of complementarity-driven and the lack of similarity-driven ties, the weak coefficients gauge the extent to which complementarity is present but also allow for the presence of similarity. In other words, strong complementarity measures bipartiteness and structural equivalence between neighbors of i as well as i and neighbors of its neighbors, while weak complementarity drops the requirement of bipartiteness.

Indeed, from the geometric perspective, the quadrangle with two chords (4-clique) can be seen as a characteristic motif for joint similarity and complementarity (Fig. 4C). Thus, weak complementarity can be high in purely similarity-driven systems, but in general it will be higher in systems driven to a significant degree by complementarity. Moreover, it also provides a measure of complementarity which is more robust to measurement errors as strong quadrangles can be easily distorted by the presence of erroneous chordal edges.

Last but not least, the relationship between weak complementarity and structural equivalence is stronger as Asymmetric Excess Sørenson Index (Eq. (11)) can be used to find both lower and upper bounds for h_i :

$$\min_{j,k,l}(H_{jk|i}, H_{il|j}) \leq h_i \leq \max_{j,k,l}(H_{jk|i}, H_{il|j}) \quad (15)$$

where j, k, l are defined over the same sets as in Eq. (12). And since we have that $c_i \leq h_i$ Eq. (15) can be used to prove the corresponding bounds for c_i from Eq. (12). See SM: S2 for the derivation and other details.

2.4. Weighted structural coefficients

Having defined all variants of the unweighted structural coefficients we can now generalize them to the case of networks with weights. This can be done in a relatively straightforward manner by weighting each triple or quadruple by the average weight of its constitutive edges. For instance, the weight of a (i, j, k) triple is equal to $(w_{ij} + w_{jk})/2$. Similarly, the weight of a (i, j, k, l) quadruple is $(w_{ij} + w_{jk} + w_{kl})/3$. Crucially, when counting triangles and quadrangles the weight of the closing edge is not used in order to ensure proper normalization in $[0, 1]$. For the same reason, in the case of weak quadrangles weights of chordal edges are ignored too. It also means that two separate weighted counts of triangles/quadrangles must be kept: one for wedge and one for head triples/quadruples (see Fig. 5). For instance, weighted similarity coefficient (denoted by adding a “hat” on top) is defined as:

$$\hat{s}_i = \frac{2T_i^W + 2T_i^H}{t_i^W + t_i^H} \quad (16)$$

where T_i^W and T_i^H are weighted counts of triangles including i using $(w_{ij} + w_{ik})/2$ and $(w_{ij} + w_{jk})/2$ for weights correspondingly. Note that if all edge weights are equal we have that $2T_i^W + 2T_i^H \propto 4T_i$ and \hat{s}_i is equivalent to its unweighted counterpart s_i . This is true for all weighted structural similarity and complementarity coefficients.

We do not repeat all the formulas for the weighted case now as, hopefully, the general logic is clear. The only change is that instead of counting triangles/quadrangles and wedge or head triples/quadruples we weight each occurrence by the average weight over edges constituting a given triple or quadruple. Detailed formulas are presented in SM in Tab. S2.

Note that this approach is not *ad hoc* and arbitrary as it can be considered a generalization of the well-known weighted clustering coefficient proposed by Barrat et al. [5]. Indeed, the weighted clustering and weighted t -clustering proposed here are equivalent. One can see this by starting from the definition of weighted t -clustering in terms of a summation over entries in the adjacency matrix:

$$\begin{aligned} \hat{s}_i^W &= \frac{\sum_{j,k} 1/2(w_{ij} + w_{ik})a_{ij}a_{ik}a_{jk}}{\sum_{j,k} 1/2(w_{ij} + w_{ik})a_{ij}a_{ik}} \\ &= \frac{\sum_{j,k} 1/2(w_{ij} + w_{ik})a_{ij}a_{ik}a_{jk}}{w_i(d_i - 1)} \end{aligned} \quad (17)$$

where w_i denotes the strength (sum of weights) of the node i . Clearly, the end result is equal to Eq. (5) in Ref. [5] which defines the weighted clustering coefficient.

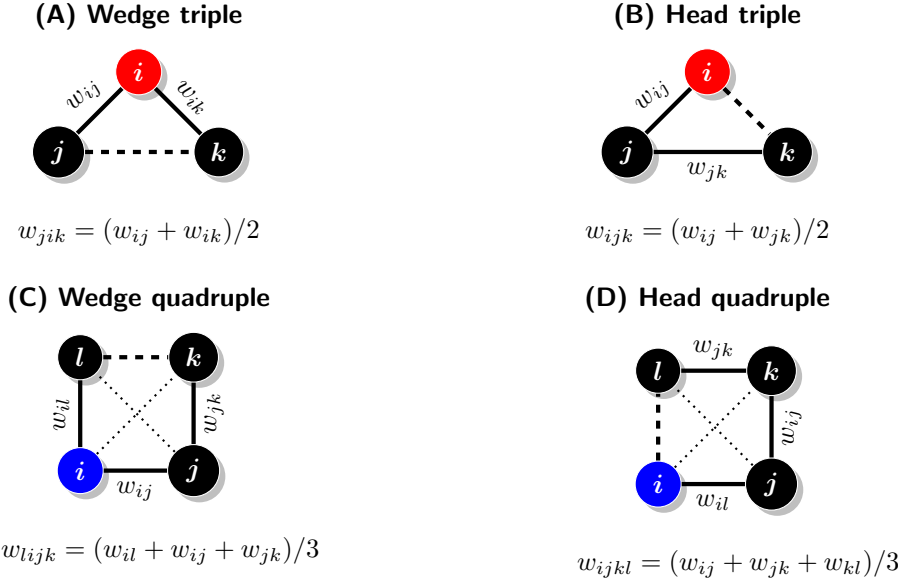


Figure 5. Weighting formulas for different kinds of triples/triangles and quadruples/quadrangles. Dashed lines correspond to edges that must exist for a given triple/quadruple to be counted as a triangle/quadrangle (but which are not included in the weight). Dotted diagonal lines denote chordal edges which are also not included in the weight of a corresponding quadruple.

2.5. Structural coefficients in random graphs

In this section we discuss the behavior of structural coefficients in some of the most important random graph models. First, let us note that in the Erdős–Rényi (ER) model [17] the expected global similarity, which is of course equivalent to global clustering, is simply $\mathbb{E}[s] = p$, or equal to the probability that any edge exists. This is a standard result that follows from the fact that for any (i, j, k) triple the closing (i, k) edge always exists with probability p [Sec. 12.4 in 36].

We can use a similar argument to derive the expected values of the global complementarity coefficients in the ER model. Let (i, j, k, l) be any connected quadruple. It forms a quadrangle with no chords if and only if the (i, l) edge exists while the (i, k) and (j, l) edges do not. Since all edges in the ER model exist independently with probability p it means that the (i, j, k, l) quadruple will make a strong (chordless) quadrangle with probability $p(1 - p)^2$. Hence, the expected value the global complementarity coefficient is $\mathbb{E}[c] = p(1 - p)^2$.

In the weak case the situation is even simpler as it is enough to have the (i, l) edge, regardless of the number of chordal edges in the (i, j, k, l) quadruple, so the expected value is $\mathbb{E}[h] = p$ and matches the expected value of the global similarity.

2.5.1. Correlations with node degrees in the configuration model

A natural null model for studying correlations of node-wise coefficients with node degrees is the configuration model in which a particular degree sequence is enforced while apart from that connections are established as randomly as possible [cf. Sec. 13.2 in 36]. In order to describe the qualitative

behavior of the node-wise structural similarity and complementarity coefficients we will use the fact that in both cases they are bounded by their corresponding clustering and closure coefficients (cf. Secs. 2.1 and 2.2). In other words, by describing the correlations between node degrees and triangle/quadrangle clustering and closure coefficients we will be able to reveal the range of possible behaviors of structural coefficients.

Firstly, let us note that it is usually conjectured that local t -clustering should generally decrease with node degree [Sec. 8.6.1 in 36]. More recently, it was analytically proven for the general family of networks with power law distributions that t -clustering is on average roughly constant for low-degree nodes and then starts to decrease more quickly as node degree grows [49].

On the other hand, the authors of local closure coefficient, or t -closure using our terminology, showed that it is positively correlated with node degree in the configuration model [54]. Thus, these two results together imply that the structural similarity coefficient, s_i , can display rich, also non-monotonic, correlations with node degree depending on the large-scale structure of a particular network.

We leave analytical study of the analogous properties of q -clustering and q -closure for future work. However, since both types of clustering and closure coefficients are very similar by construction — in the first case the closing link is between two (in)direct neighbors of i while in the second it is between i and one of its (in)direct neighbors — we conjecture that they should display the same qualitative behavior in the configuration model. More concretely, we expect that q -clustering should decrease with node degree, especially for well-connected nodes, and q -closure should increase with node degree. As a result, we also expect that the structural complementarity should be able to vary with respect to node degree in various, also non-monotonic, ways.

We validate the above reasoning on a set of four real-world networks from different domains: 1) Jazz collaborations (offline social); 2) Combined friendship network made of 10 samples of ego-nets from Facebook (online social); 3) Human Protein Interactome (biological); 4) Internet at the level of Autonomous System (technological) (see Secs. 4.3.2 and 4.3.5-4.3.7, for details).

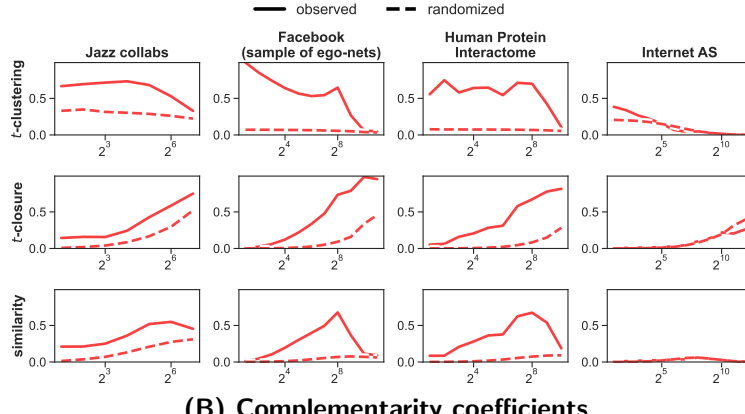
We study correlations between various similarity and complementarity coefficients by plotting their averaged values against node degrees using logarithmic binning with base 2. Moreover, we also plot corresponding averages calculated based on 100 randomized replicates sampled from Undirected Binary Configuration Model (UBCM) (see Ref. [48] and Sec. 4.4.1 for details).

As evident on Fig. 6, the general qualitative behavior of all similarity- and complementarity-related coefficients in randomized networks agrees with the theoretical expectations. Both clustering coefficients tend to be either roughly constant or decrease with node degree in randomized networks. Their behavior in real, observed networks is more nuanced, but in most of the cases follows similar correlation patterns, even if the actual observed values of coefficients are very different. Similarly, both closure coefficients tend to increase with node degrees in both randomized and observed networks suggesting that this correlation may be quite universal.

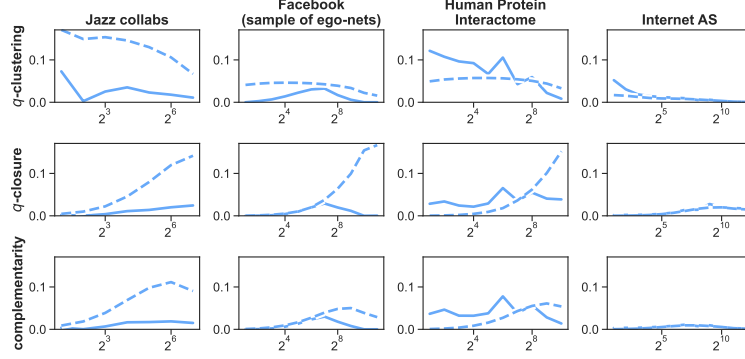
Similarity and complementarity coefficients in randomized networks tend to follow a path more similar to closure coefficients, but the increase for high degree node is much less pronounced or the coefficients start to decrease slightly. On the other hand in many of the observed networks they display more complex, non-monotonic behavior. In other words, the analysis strongly suggests that the theoretical expectations discussed earlier are reasonable and capture much of the trends that can be seen in empirical data.

Interestingly, the analysis points also to some potential differences in terms of the importance of similarity and complementarity in different types of networks. Not surprisingly, all observed similarity-related coefficients are much higher than their randomized counterparts in social networks

(A) Similarity coefficients



(B) Complementarity coefficients



(C) Weak complementarity coefficients

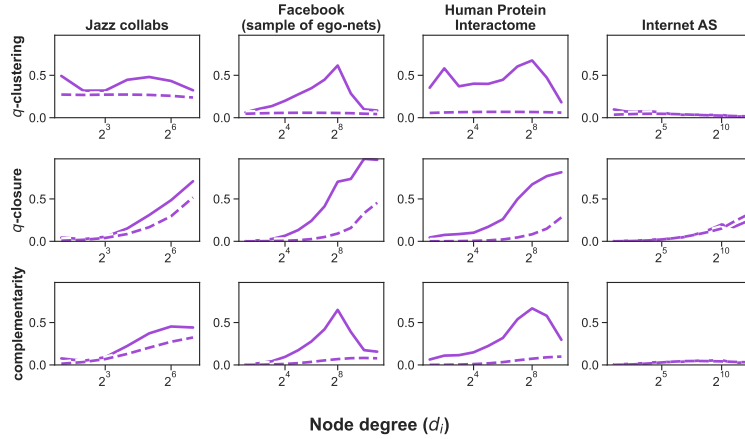


Figure 6. Observed and randomized values of similarity and complementarity coefficients in four real-world networks as a function of node degree agree with the theoretical expectations. Values are averaged in logarithmic bins (with base 2). Dashed lines represent averages based on 100 randomized replicates sampled from Undirected Binary Configuration Model (UBCM).

(Jazz collaborations and Facebook ego-nets; see Fig. 6A). On the other hand, the observed values of complementarity-related coefficients are much closer to the expectations based on the configuration model or even lower (Fig. 6B-6C). This is especially true for the offline social network of jazz collaborations, while in the online network of Facebook ego-nets the observed values of the weak coefficients using the relaxed definition of quadrangles allowing for chordal edges are markedly higher than their randomized counterparts. In other words, the two networks, while driven primarily by similarity, have somewhat different mesoscopic structures. This suggests that perhaps social processes shaping offline and online social networks may differ to some extent, which would not be too surprising as interactions on online platforms are mediated through technological infrastructure. In particular, our results suggest that in online social networks the homophily pressure may be strong enough to induce not only similarity between the ego and its 1-hop neighbors but also structural equivalence with respect to 2-hop neighbors. This is of course a tentative hypothesis which needs to be tested using a richer empirical material, but, importantly, it is structural coefficients that we propose which facilitate asking such a question.

The relationship between the coefficients and node degrees in the interactome network are quite similar to those observed for the offline social network. However, in this case it seems that the values of complementarity-related coefficients are increased for low-degree nodes even in the case of the measures based on strong quadrangles indicating that connections around peripheral nodes may be to some extent driven by complementarity.

Last but not least, in the network of the Internet at the level of Autonomous System the observed values of both similarity- and complementarity-related coefficients are almost indistinguishable from their randomized counterparts. In other words, it seems its structure is neither driven by similarity nor complementarity.

Summing up, the results suggest that networks from different domains may differ in systematic ways in terms of the extent to which they are shaped by similarity or complementarity. We return to this problem in Sec. 2.7.

2.6. Discriminating between similarity- and complementarity-driven networks

We now turn to the question of the theoretical validity of the proposed coefficients. In other words, we want to test whether our measures are related to meaningful, interpretable phenomena.

For this purpose, we focus on an application in the domain of sociology and social networks analysis [51]. The question is whether the structural coefficients can be used to discriminate between different types of social relations. To answer it, we use a set of (undirected and unweighted) social networks collected by Chami et al. [13] in 17 rural villages in Mayuge District, Uganda. For each village two networks of relations between households were measured: 1) a friendship network and 2) a health advice network (see Sec. 4.3.1 for more details).

This dataset provides a perfect opportunity for empirical testing of the theoretical validity of our approach as it is sociologically justified to consider the two types of networks as driven by different generating mechanisms. It is a well documented fact that friendship relations are to a large extent driven by homophily, or similarity, between different persons [2, 27, 32, 34]. On the other hand, health advice networks should be at least partially driven by complementarity, as the act of advice is usually based on a difference in knowledge or information between an adviser and an advisee. Of course, the structure of health advice networks can still be expected to be partially influenced by homophily as well as various other processes as real networks are hardly ever products

of a single generating mechanism. However, if the proposed theory is true, there should be some kind of statistical signature of complementarity present in their structure.

In this context it is natural to expect that both global and node-averaged similarity coefficients (s and $\langle s_i \rangle$) should be typically higher in friendship networks. On the other hand, the analogous complementarity coefficients (c and $\langle c_i \rangle$) should be on average higher in health advice networks, and this should hold also for the weak coefficients (h and $\langle h_i \rangle$), although perhaps to a lesser extent.

Fig. 7A presents distributions of values of all the aforementioned coefficients. The pattern of differences is not systematic and partially contrary to our hypothesis. The similarity coefficients are higher in the friendship networks which seems to confirm it. However, strong complementarity also seems to be higher in the friendship networks which is contrary to our expectations. Only global weak complementarity appears to be higher in the health advice networks.

Note, however, that the two types of networks have on average markedly different degree distributions as indicated by average degrees and coefficients of variation (Fig. 7B). Moreover, structure induced by complementarity may be hidden and distorted by other processes such as homophily, especially as quadrangles are in general higher order motifs than triangles (they consist of 4 nodes instead of 3). Because of that, we conducted also an analysis using values calibrated against a null distribution based on Undirected Binary Configuration Model (UBCM) (see Sec. 4.4.1 for details) which randomizes network structure while fixing the expected degree sequence. This allowed controlling for the observed differences between first-order structure of friendship and health advice networks.

For each observed network 500 randomized replicates were sampled from UBCM and the average ratios of the observed and randomized values of the coefficients were calculated. Fig. 7C shows distributions of the calibrated coefficients (in \log_2 scale) together with average relative differences between friendship and health advice networks as well as associated p -values corrected for multiple testing using Holm-Bonferroni method. Statistical significance was assessed using one sample t test (with two-sided null hypothesis) conducted on differences between the average log-ratios for subsequent pairs of friendship and health advice networks from the same villages.

As evident in Fig. 7C, the adjusted results are in clear agreement with the theoretical expectations. For both similarity coefficients friendship networks have typically increased values (log-ratios greater than zero) and the mean differences are statistically significant at $p \leq 0.001$. On the other hand, the results for complementarity coefficients are exactly opposite and in this case health advice networks have significantly larger calibrated values with all mean differences significant at least at $p \leq 0.05$. Moreover, effect sizes are smaller for weak complementarity coefficients, which agrees with the interpretation that weak quadrangles with one or two chords correspond to relations in which complementarity is combined with increasing amounts of similarity.

In summary, the results confirm that similarity- and complementarity-driven networks have specific structural signatures which can be statistically detected, at least when a proper care and adjustments are used. In order to gauge the discriminatory power of the coefficients better, we fitted also a simple supervised classifier based on Quadratic Discriminant Analysis (QDA) [Sec. 4.3 in 21] using only two predictors: average node similarity and complementarity coefficients (this pair yielded the best prediction quality). The out-of-sample accuracy of the model estimated with 17-fold stratified cross-validation (one fold per village) was 85.29% (see Fig. 7D), which provides further confirmation of the theoretical validity of our approach.

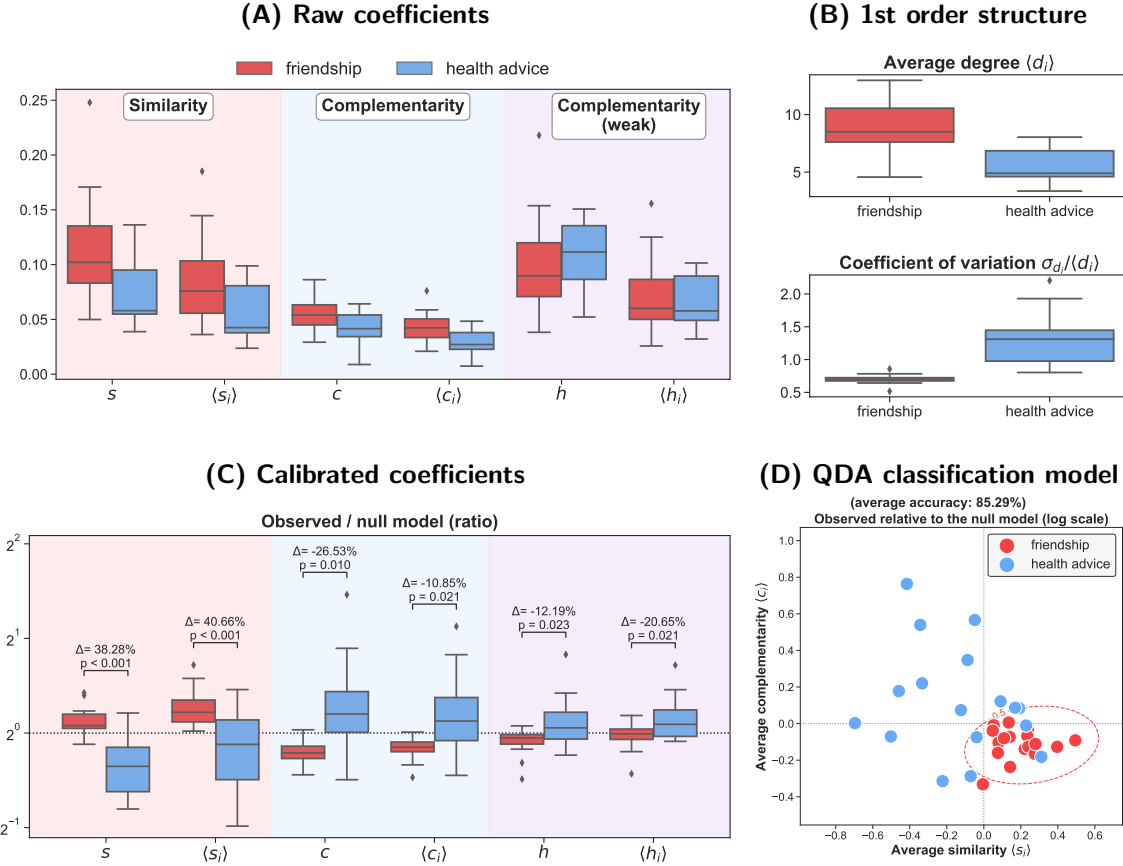


Figure 7. Comparison of structural coefficients between friendship and health advice networks in 17 Ugandan villages. Structural coefficients calibrated against the null model accounting for differences in terms of first-order structure discriminate between friendship and health advice networks. **(A)** Distribution of raw coefficients. **(B)** Average first-order structure of the two types of networks as quantified through average degrees and coefficients of variation of degree distributions. **(C)** Comparison of structural coefficients relative to the null model (in \log_2 scale) based on 500 samples from UBCM with estimated average relative differences between friendship and health advice networks in terms of the average logarithms of the ratios of observed and randomized values (Δ) as well as associated p -values for t -tests adjusted using Holm-Bonferroni method. **(D)** Bivariate distribution of logarithms of average similarity and (strong) complementarity coefficients calibrated against the null model distribution with the decision boundary separating friendship and health advice networks (marked in red) based on Quadratic Discriminant Analysis (QDA).

2.7. Structural coefficients in networks from different domains

After confirming the theoretical validity of our approach we now return to the question of whether real-world networks from different domains tend to differ systematically in terms of the extent to which their structure is driven by similarity and complementarity. We study this problem based on four network datasets from different domains (see Secs. 4.3.2 and 4.3.1-4.3.4 for details):

1. **Social (offline).** 34 Ugandan friendship and health advice networks.
2. **Social (online).** 10 ego networks sampled from Facebook together with a joint network combining all ten samples.
3. **Biological.** 10 networks of protein-protein interactions in *C. elegans* measured using different methods and approaches.
4. **Technological.** 17 networks of dependencies between programming languages/software projects.

For each network both global and node-averaged similarity and complementarity coefficients (strong and weak) were calculated. Additionally, we calibrated the observed values against an appropriate null distribution based on 100 samples from UBCM (see Sec. 4.4.1). For each UBCM sample the log-ratio of the observed and the randomized values was computed and then the average over all samples was taken (the same approach as in Sec. 2.6). Then, in order to avoid overfitting and facilitate visualization the calculated coefficients (raw and calibrated separately) were projected onto two-dimensional subspace using Principal Component Analysis (PCA). Finally, PCA-projected scores were used as features in Quadratic Discriminant Analysis (QDA) which was used for domain classification. Out-of-sample accuracy was estimated with 5-fold stratified cross-validation.

Figs. 8A and 8B present the results of analyses based on raw and calibrated coefficients correspondingly, with cross-validated accuracy scores (percentages of correctly classified observations) and dashed lines denoting decision boundaries for different classes (domains). The decision boundaries for biological networks are not shown, as this was the only class with a heterogeneous and scattered distribution of the structural coefficients.

The top panels on Fig. 8 show PCA loadings or linear correlations between individual structural coefficients and principal components. Apparently, in both cases there is a distinction between dimensions corresponding to similarity (loaded primarily by similarity and weak complementarity coefficients) and those related to complementarity (loaded primarily by strong complementarity). However, the pattern is much clearer for the calibrated coefficients.

In general the results based on the raw and calibrated coefficients are qualitatively very similar. However, in the first case it is differences in terms of similarity dimension that are most important (correspond to 90.67% of the variance), while for the calibrated coefficients the complementarity dimension is more important and reproduces 53.69% of the original variance. This is understandable as measuring complementarity depends on motifs of higher order than similarity (4 nodes instead of 3). Hence, without a proper calibration raw values of complementarity coefficients may be often lower and more noisy. Thus, calibrated coefficients may be easier to interpret and generally more useful.

Note that the scatterplots on Fig. 8 show PCA-projected data so positions along the PCA dimensions should be interpreted as relative to other data points. For instance, a low score on the similarity axis does not necessarily mean that similarity coefficients of this network are low in absolute terms but rather relative to other networks.

The bottom panels show cross-validated accuracy scores for analogous models based on subsequent subsets of the coefficients (with the last category corresponding to the main model). They indicate that networks from different domains can be separated relatively well even using only similarity coefficients, but the addition of complementarity coefficients markedly increases the accuracy. In the case of the raw coefficients it is weak complementarity that improves the performance the most (adding strong coefficients seems to decrease it slightly), while in the case of the calibrated coefficients it is already strong coefficients that yield the largest improvement. Again, this is due

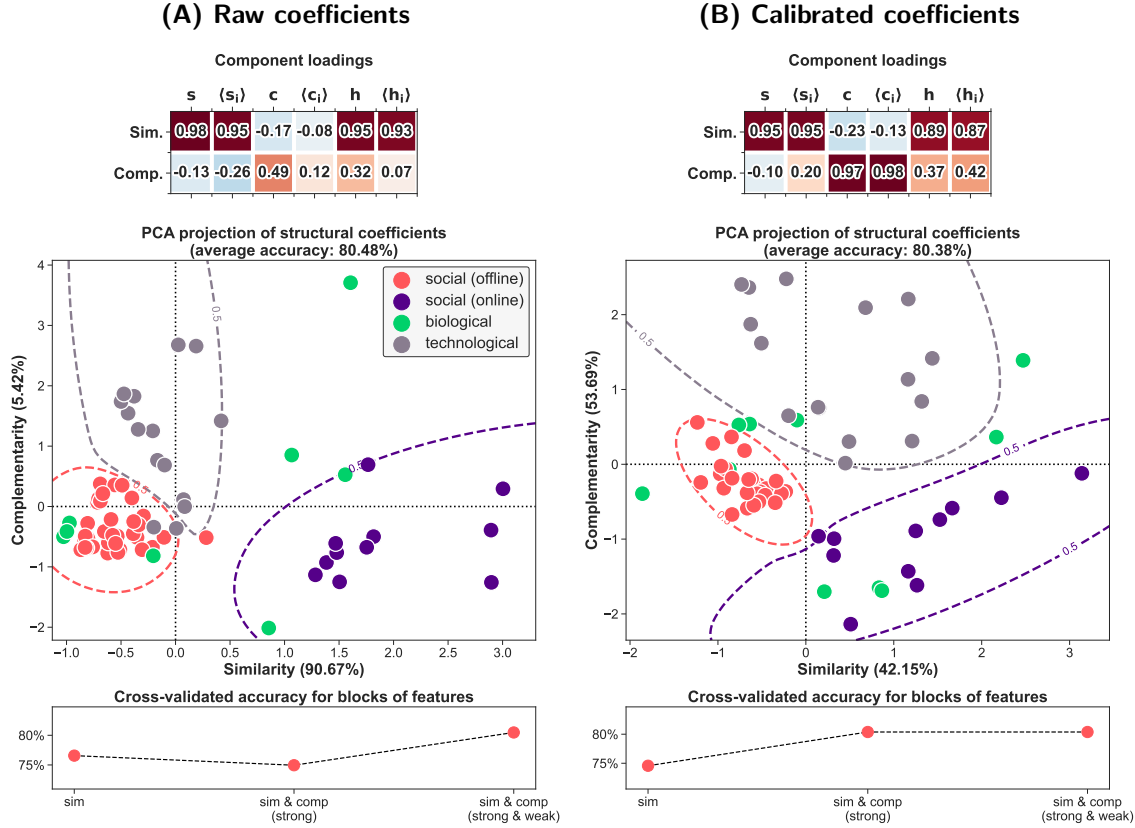


Figure 8. Classification of network domains based on a PCA-projection of structural coefficients. The top panels show correlations between the coefficients and principal components. Dashed lines on the scatterplot show decision boundaries based on QDA model for different classes excluding the biological networks with a very heterogeneous distribution. Shares of the variance retained by components are shown on the axes labels. The bottom panels show cross-validated accuracy scores for different subsets of input features. **(A)** Analysis based on raw coefficients. **(B)** Analysis based on coefficients calibrated against a null distribution based on 100 samples from UBCM.

to the fact that in many real-world networks raw values of complementarity coefficients may not be that informative as strong quadrangles are sensitive to noise and overlap with other generative processes such as similarity.

More generally, our analysis indicates that online social networks are on average driven by similarity to a larger extent than other networks, which is not surprising as, being purely friendship networks, they are very likely to be shaped by the principle of homophily [34]. On the other hand, technological networks of software dependencies are relatively more driven by complementarity. To our best knowledge, there is no general theoretical principle that would predict such an outcome but nonetheless the result seems to be rather reasonable. For instance, two software programs solving

similar problems will hardly ever depend on each other but may share a lot of other dependencies leading to the emergence of quadrangles and locally bipartite-like subgraphs in general.

Somewhat surprisingly, offline social networks in our analysis tend to be relatively low on both similarity and complementarity dimensions. This result may be specific for the particular dataset we used. However, it also suggests that a large-scale analysis of structural differences between offline and online social networks based on more diverse data could be an interesting problem to study. Last but not least, interactomes (biological networks) are most heterogeneous and scattered all over the space spanned by the principal components meaning that some of them are to a relatively large extent driven by similarity, some by complementarity and some by neither or both.

To sum up, the analysis shows that different types of real-world networks may have different characteristic levels of structural similarity and complementarity coefficients. This, in turn, suggests that their structure may be shaped to different extent by similarities and complementarities between nodes, pointing to possible qualitative differences in terms of their underlying domain-specific generating mechanisms.

2.8. Detection of groups of structurally similar or complementary nodes

For the last case study we turn to the problem of the detection of pairs, and possibly also groups, of nodes which are structurally similar and/or complementary. This will serve as an illustration of the utility of the edge-wise structural coefficients. Moreover, for the empirical material we will use an undirected but weighted network in order to show that the weighted structural coefficients perform better at capturing and summarizing structure of networks in the presence of edge weights.

We analyze a network of co-appereances of characters in *A Storm of Swords* novel in which edge weights indicate the number of times any two characters appeared in the text within at most 15 words from each other [7] (also see Sec. 4.3.8). *A Storm of Swords* is the third book in *A Song of Ice and Fire* series, a hugely popular epic fantasy saga by George R. R. Martin, which was catapulted to even greater world-wide fame after being adapted to small screen by HBO as a hit TV series *Game of Thrones*.

We chose this network for several reasons: 1) it is an undirected weighted network which provides us with an opportunity to illustrate the utility of the weighted structural coefficients; 2) it is relatively small which makes qualitative interpretation of quantitative results easier; 3) the represented world of *A Song of Ice and Fire* saga is known for its creation of complex characters and plotlines inspired by the history of medieval Europe and was shown to display realistic measures of social complexity [18]. Thus, it may be expected that the pattern of connections between characters encodes information related to how they are embedded within the intricate social and political structures of the represented world.

The main question we ask here is: can pairs, and possibly groups, of structurally similar and/or complementary characters be identified using the edge-wise structural coefficients and whether does the information on connections' weights play a role in this setting? Generally speaking, structurally similar characters are those who share ties with more or less the same set of others. On the other hand, two characters are structurally complementary if their associates are often connected to each other.

In a preliminary step of the analysis we calculated unweighted (weighted) node-wise similarity and complementarity coefficients and plotted them as a function of node degrees (strengths). Moreover, the observed values were contrasted with their randomized counterparts based on 200 samples from UBCM in the unweighted case and Undirected Enhanced Configuration Model (UECM; see

Sec. 4.4.2) in the weighted case. Note that UECM is a configuration model inducing the maximum entropy probability distribution with specific expected node degree and strength sequences and assuming that edge weights are arbitrary positive integers, which is a correct assumption for a network of co-appearances.

The upper right panels on Figs. 9A and 9B show that both the unweighted and weighted structure of the network is similar in terms of the correlations between node-wise similarity or complementarity and node degrees/strengths. The observed levels of similarity are markedly higher than the null model expectations over the entire degree/strength spectrum, indicating that the network structure is driven primarily by similarity. However, weak complementarity is also somewhat increased relative to null model averages, suggesting that when two characters are connected then their associates are likely to be connected too. This is not very surprising considering the fact that characters are clustered not only due to their allegiances and roles but also within the well-defined geography of the represented world (more on this below). Moreover, both similarity and weak complementarity grow quite quickly with increasing node degree/strength indicating that most central characters in the network are surrounded by relatively tightly knit groups of associates. On the other hand, observed values of strong complementarity are very low and markedly lower than their null model counterparts indicating that it is similarity that drives the system and that the increased levels of weak complementarity are induced rather by a strong pressure on structural similarity than genuine, pure complementarity. In other words, there is no evidence of dense bipartite-like subgraphs.

Next, we calculated observed unweighted and weighted edge-wise structural similarity and complementarity coefficients (strong and weak) and estimated their corresponding p -values by comparing against a simulated null model distribution based on UBCM (unweighted) or UECM (weighted). In order to have at least 100 samples per each unique combination of sufficient statistics we coarse-grained observed values of sufficient statistics using logarithmic binning (with base 2) and generated 2000 samples from UBCM and 8000 samples from UECM (see Sec. 4.5 for details). Then, we found groups of structurally similar/complementary characters using the following procedure: 1) choose significance level α and filter out all edges with $p > \alpha$ for all three structural coefficients (Benjamini-Hochberg FDR correction for multiple testing was used [6]); 2) decompose the filtered network into components and assign all nodes in the same component to the same cluster; 3) calculate modularity score for the partition on the unfiltered network; 4) repeat steps 1-3 for $\alpha = 0.01, 0.02, \dots, 0.99$ and choose the value maximizing modularity. Finally, communities consisting of less than three nodes were combined in one class of outliers (marked in white on Fig. 9).

It is important to stress at this point that the present analysis is meant to be rather a proof-of-concept study aimed at showing that the structural coefficients capture meaningful mesoscopic properties of networks rather than claiming that the above naive procedure is a statistically optimal community detection method. Firstly, it does not produce a proper partition due to the possible presence of the “outlier” cluster. Secondly, its main aim is to detect pairs of significantly similar/complementary nodes, and the detection of groups of such nodes is achieved only as a potentially useful byproduct of the main goal. Thirdly, as a community detection method it can be viewed as an intermediate instance between descriptive methods based on intuitive heuristics and inferential ones informed by explicitly formulated generative models (we use this distinction in the sense proposed in Ref. [39]) More concretely, statistical significance of edge-wise coefficients is based explicitly on a plausible null model, but the procedure for maximizing modularity is not informed directly by an explicit statistical model and thus may be suboptimal and prone to overfitting. Nonetheless, as we show below, in the present case study the agreement between our method

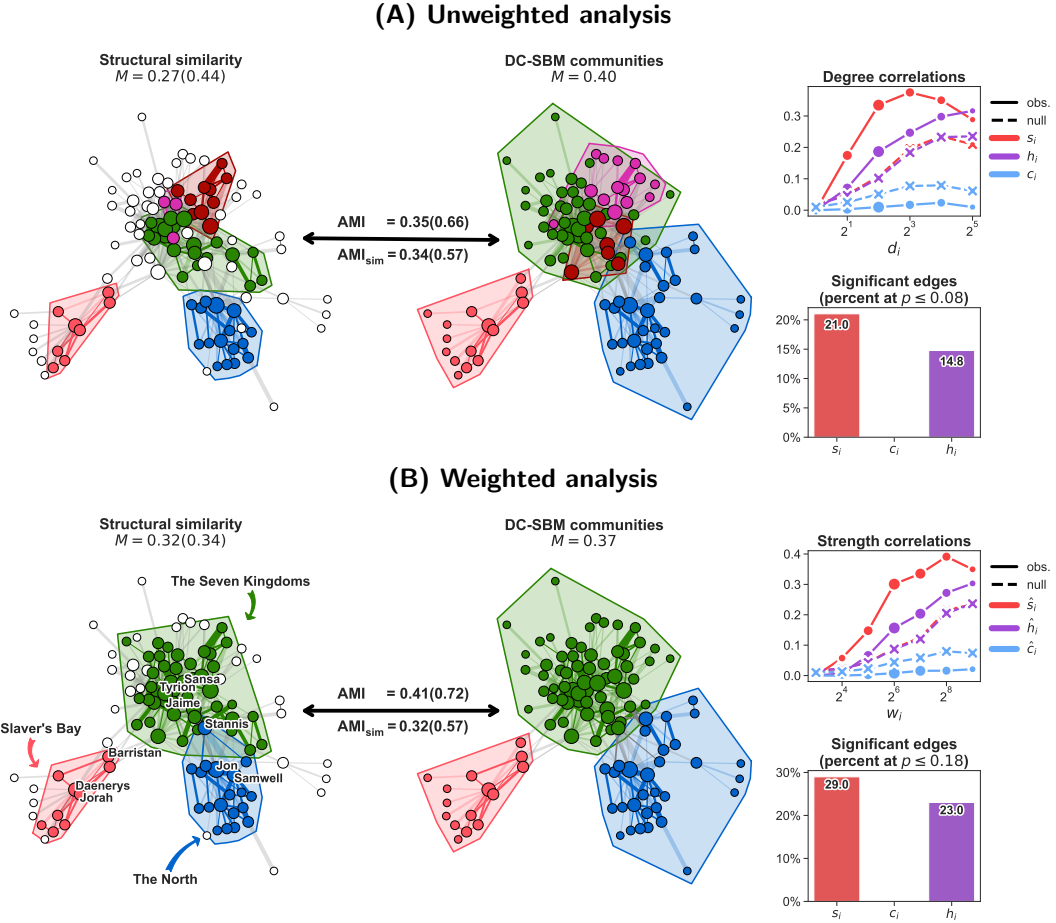


Figure 9. Structural coefficients and detection of structurally similar nodes in the character co-appearance network of A Storm of Swords. Weighted coefficients yield better partition which is more aligned with the communities detected with DC-SBM. **(A)** Unweighted analysis. The left network presents groups of structurally similar actors with outlier nodes marked in white and the right network shows the best partition estimated with DC-SBM (over 100 repetitions). Modularity scores (M) are reported under the network labels and the similarity of network partitions are measured with AMI scores calculated separately for detection based on all edge-wise structural coefficients and only the similarity coefficients (AMI_{sim}). The values in parentheses correspond to modularity and AMI scores calculated after removing outlier nodes. The upper right panel shows average values of structural coefficients as a function of node degree for the observed network and the corresponding null model expectations based on 200 samples from UBCM. The lower right panel shows fractions of significant edges for different structural coefficients. **(B)** As above but using weighted coefficients. Coefficients are plotted against node strengths and UECM is used as null model. DC-SBM in this case assumed geometric distribution of weights. Three nodes with highest strengths per group of structurally similar characters are labeled and groups are named according to their qualitative interpretation.

and the results of an inferential community detection based on Degree Corrected Stochastic Block Model (DC-SBM) [37] is quite high, in particular when information on edge weights is used. Moreover, in SM: S5 we present a preliminary analysis suggesting that the proposed method can be robust against overfitting and does not detect spurious groups in random networks.

In the unweighted case the significance threshold maximizing the modularity score was $\alpha = 0.08$ (see the bottom right panel of Fig. 9A), leading to 21% of edges with significantly high structural similarity and 14.8% with significant weak complementarity. Remarkably, no edges displayed significantly high strong complementarity which agrees with our previous conclusion regarding the lack of bipartite-like substructures within the network. However, relatively many nodes were assigned to the outlier cluster and the groups of structurally similar characters revealed in this analysis were rather small and only moderately similar to the communities detected with DC-SBM (also unweighted) as quantified using Adjusted Mutual Information (AMI) score [50]. Also modularity of the partition was markedly lower than the modularity of the optimal partition based on DC-SBM ($M = 0.27$ vs $M = 0.40$). The values in parentheses on Fig. 9A are modularity and AMI scores calculated on the subgraph obtained by removing outlier nodes. Moreover, AMI_{sim} measures the clustering similarity for a partition using only structural similarity coefficient. Clearly, in this case it is very similar to the main AMI score indicating that when edge weights are discarded the additional information provided by weak complementarity is negligible.

In the weighted case the significance threshold was $\alpha = 0.18$ and 29% of edges had significantly high similarity and 23% high weak complementarity (see the lower right panel in Fig. 9B). The modularity of the obtained partition was in this case higher ($M = 0.32$) and closer to the modularity score of $M = 0.37$ obtained by DC-SBM (which in this case incorporated edge weights sampled from a geometric distribution). Moreover, AMI scores were generally higher indicating better agreement between the obtained partitions, which, arguably, can be also confirmed visually on Fig. 9B. The improvement of the AMI score relative to AMI_{sim} is also much higher, indicating that weak complementarity coefficients provided some useful information in this case. Thus, the results suggest that by using information on edge weights the detected groups of structurally similar characters were of better quality, in particular when compared to a partition based on a weighted DC-SBM. Thus, we will now present a qualitative interpretation of the results only for the weighted analysis.

Remarkably, both the proposed method based on structural coefficients and DC-SBM revealed partitions into three, largely similar, communities (ignoring the outlier nodes) which quite clearly correspond to the three main plotlines and geographical regions of the represented world of *A Storm of Swords*¹. The largest cluster, named “The Seven Kingdoms” and marked in green on Fig. 9B, corresponds to characters involved in political struggles and intrigues taking place within the Seven Kingdoms, that is, the political organism at the center of the overarching narrative, for it is the fight between various noble houses for the Iron Throne of the Seven Kingdoms that animates the complex political landscape depicted in the saga. The second cluster, named “The North” and marked in blue, groups characters thrown by fate to the far north where they guard the known world from hosts of barbarians and demonic creatures. The third and last cluster, named “Slaver’s Bay” and marked in orange, corresponds to the exiled queen Daenerys and her closest allies and entourage, who, after conquering merchant cities in the region known as Slaver’s Bay and effectively abolishing slave trade, prepare her forces for crossing the sea and invading the Seven Kingdoms to reclaim the Iron Throne. For the sake of legibility, Fig. 9B shows labels of only three characters

¹See https://en.wikipedia.org/wiki/A_Storm_of_Swords for the plot summary. Accessed: December 21, 2021.

with highest sums of weights in each group, but network plots with labels for all nodes are presented in SM: [S6](#).

Summing up, the results show that edge-wise structural coefficients can be used to detect pairs and groups of structurally similar/complementary nodes and that such groups can correspond to qualitatively meaningful partitions of a network which are comparable to results of state-of-the-art community detection methods such as DC-SBM [37]. Moreover, the weighted structural coefficients can capture important information about topology of the network leading to better results relative to those produced using their unweighted counterparts.

3. Discussion

We have introduced two general families of graph-theoretical coefficients for measuring the extent to which relations are driven by similarity and/or complementarity that can be calculated at the level of edges, nodes and entire graphs. The measures we propose can be applied to undirected networks with or without edge weights. They are defined in purely combinatorial manner, that is, in terms of counts of different kinds of paths (triples and quadruples) and cycles (triangles and quadrangles). However, they are motivated by geometric arguments which can be used to extend models developed within the emerging field of network geometry (see Ref. [8] for a recent overview) to systems driven not only by similarity but also complementarity. Indeed, the present work stemmed from our considerations of network geometry going beyond the principle of similarity and we hope that it will prove to be of value in informing a new generation of latent space models. In particular, we believe that the idea of linking different kinds of organizing principles and generating mechanisms, such as similarity or complementarity, to their characteristic network motifs (e.g. triangles and quadrangles) may turn out to be especially useful. Moreover, we believe that structural coefficients can be useful for validating different kinds of latent space models. In particular, complementarity coefficients can be used to test whether a geometric model of complementarity-driven relations really generates networks with locally dense bipartite-like subgraphs.

While we are aware of the complexities associated with the term “structural” in the network science literature, for instance in the context of graph or node distance/similarity metrics (see Refs. [20, 43] for an overview of these rich topics), we still argue that the measures we propose can be meaningfully called *structural coefficients*. We think so for two reasons: 1) they are defined mathematically purely in terms of observable network structure or without any reference to node or edge attributes (observed or latent); 2) as we show in Secs. 2.1.1 and 2.2.1 they are directly linked to the fundamental notion of structural equivalence [36, 51]. In other words, they really measure the extent to which the structure at the level of a given edge, node or graph is driven by similarity and/or complementarity.

The proposed family of structural similarity coefficients is built on top of classical local clustering [52] and more recent local closure [54] coefficients. Crucially, it combines these two perspectives in one general measure which captures two different aspects of the fundamental triadic closure process: 1) the tendency of “friends” of ego to connect to each other; 2) and the analogous tendency of ego to connect to “friends of its friends”. Moreover, as we show, structural similarity at the level of a node is maximal if and only if the node belongs to a fully connected network. This links our notion of structural similarity directly to a classical result from structural balance theory, namely, the discovery that for a network to be perfectly clusterable it either has to be fully connected or decomposed into multiple fully connected components [16]. In other words, this suggests that too

strong a pressure on structural similarity, assuming fixed average degree, must inevitably lead to a decomposition of a system into disconnected parts. We believe that this result may be useful for studies on polarization and social fragmentation [4, 40].

On the other hand, the family of complementarity coefficients, based on counting quadrangles instead of triangles, can be used to measure how dense and bipartite-like are structures at different levels. When limited to the domain of purely bipartite networks the coefficients can be viewed simply as a variation of the bipartite clustering coefficient [55]. However, the crux is that the distinction between purely unipartite and bipartite networks is often too sharp and, we argue, network science needs measures for quantifying local bipartiteness. But this should not be done by simply checking whether a given subgraph is bipartite-like, as tree-like subgraphs are also bipartite-like. Instead, a proper measure should account for both bipartiteness and density in order to rule out simpler tree-like structures and this is exactly what is captured by structural complementarity coefficients. Crucially, since bipartite networks are composed of two distinct kinds of entities with connections going only between them, they are complementarity-driven systems *par excellence*. This justifies the interpretation of our coefficients in terms of structural complementarity.

The connection between complementarity and bipartiteness implied by structural coefficients emerges naturally also in other contexts such as games on graphs. One of many types of games studied in game theory are so-called complementarity games which are used to model problems with negative externalities, that is, such in which the higher the number of players choosing a particular strategy the lower the payoff. Remarkably, it has been shown that if a complementarity game is played on a bipartite graph the equilibrium does not depend on payoffs associated with different strategies. It is fully determined by the structure of the network [12]. This result not only validates our analysis which links complementarity and bipartiteness but also suggests that complementarity-driven relations may be characteristic for systems and processes characterized by negative externalities.

Complementarity is also about the abundance of 4-cycles. As we showed, this is closely connected to the level of structural equivalence between neighbors of a node and the node and neighbors of its neighbors. In some cases this kind of structural equivalence may be of interest in itself, that is, without an additional requirement of local bipartiteness. This is why we propose also the family of weak complementarity coefficients based on the notion of weak quadrangles allowing for the presence of chordal edges which relaxes the bipartiteness assumption. As we argue, they can be useful for describing systems with multiple overlapping generating mechanisms and especially those driven by both similarity and complementarity. Furthermore, they can also provide a measure of complementarity more robust to measurement errors.

Furthermore, we studied theoretical validity and practical utility of the structural coefficients on a rich empirical material. In Sec. 2.5 we studied expected values of structural coefficients in various random graph models and in particular their correlations with node degrees in the configuration model and compared the null model behavior with trends observed in several real-world networks from different domains. We also showed that structural coefficients can be used to discriminate between different kinds of social relations such as friendship and health advice (Sec. 2.6) as well as real-world networks from different domains from online social networks to software dependencies (Sec. 2.7). In Sec. 2.8 we showed that the edge-wise structural coefficients can be used to detect groups of structurally similar/complementary nodes, while avoiding overfitting and finding spurious clusters in noise. The results were comparable to partitions found with a state-of-the-art community detection algorithm [37] and had a meaningful qualitative interpretation. Moreover, our analysis

indicates that the weighted variants of structural coefficients indeed lead to better results in the presence of edge weights.

Last but not least, we designed efficient algorithms for calculating unweighted and weighted structural coefficients that can be viewed as a special case of the state-of-the-art graphlet counting algorithm [1] (see Sec. 4.1). In other words, their asymptotic worst-case computational complexity matches the best available methods solving similar problems. The algorithms, together with a suite of auxiliary methods, will be distributed as a Python package through *Python Package Index* upon publication.

Our empirical analyses were based on an extensive use of null models in the form of soft configuration models formalized within the framework of Exponential Random Graph Models (ERGM) (see Ref. [42] for an overview). We argue that this is an appropriate approach for calibrating observed values of structural coefficients in a way that accounts for effects induced purely by first-order structure (e.g. degree sequence). On a more practical level, our approach was based on comparisons between observed values and null distributions simulated by sampling multiple randomized versions of an observed network from an appropriate configuration model. This method works well for global or node-level statistics, but becomes very computationally expensive when edge-wise coefficients are of interest. Therefore, analytical methods for determining null distributions of edge-wise structural coefficients could be of great value and we believe it is worthwhile to address this problem in the future.

Another obvious limitation is the fact that our methods cannot be applied to directed networks. Of course, any directed network can be interpreted as an undirected network (this is how we interpreted the software dependencies graphs in our analysis of real-world networks from different domains). However, regardless of how it is done, some part of the topological information is lost in translation. On the other hand, the geometric motivation of structural coefficients as well as most of latent space models are inherently undirected, so it is not immediately clear how directed coefficients could be defined. For now, we leave it as an interesting open problem.

In summary, in this paper we defined a set of graph-theoretic coefficients for measuring relations driven by similarity and/or complementarity that are motivated by geometric considerations. We designed efficient algorithms for calculating them and validated their theoretical validity and practical utility on a rich empirical material. We hope that the structural coefficients we propose will be a valuable addition to the toolbox of network science and that in time they may become as fundamental and widely used measures for describing mesoscopic and macroscopic structural properties as local and global clustering coefficients.

4. Materials and methods

4.1. Computing structural coefficients

Structural coefficients are based on counting triples and triangles (similarity) and quadruples and quadrangles (complementarity). While the first problem is relatively easy and efficient methods for solving it are implemented in most of popular libraries for graph-theoretical computations, the second problem of counting quadruples and quadrangles is more difficult and corresponding efficient algorithms are not widely known. Here we solve both problems by counting all motifs of interest at the level of individual edges and then aggregate the edge-wise counts to node-wise or global counts when necessary. We propose an algorithm which can be seen as a special case of the state-of-the-art graphlet counting method proposed in Ref. [1]. We also generalize it to the case of weighted

relations. Pseudocode for both algorithms is presented in SM: [S3](#). We call them **PathCensus** algorithms as ultimately they count how often different types of paths and cycles occur in a given network.

Crucially, the algorithms calculate only path and cycle counts at the level of edges. Node and global counts can be obtained by aggregating edge counts. The rules of aggregation are summarized in Tab. 1. Once the edge counts are known the aggregation formulas can be used to calculate values that can be substituted directly to equations defining structural coefficients such as Eq. (3). In the weighted case there are separate counts of triangles/quadrangles for wedge and head triples/quadruples (see SM: [S3.2](#)). However, the aggregation rules remain the same, they are just applied separately to different variants. Tabs. [S1](#) and [S2](#) in SM present detailed formulas for all structural coefficients expressed in terms of the aggregated counts.

Table 1. Notation summary and formulas for aggregating from edge to node and global counts

		Counting level				
	Edge	Node	Global			
Paths						
Wedge triples	t_{ij}^W	$t_i^W = \sum_j t_{ij}^W$	$t^W = \frac{1}{2} \sum_{i,j} t_{ij}^W$			
Head triples	t_{ij}^H	$t_i^H = \sum_j t_{ij}^H$	$t^H = \frac{1}{2} \sum_{i,j} t_{ij}^H$			
Wedge quadruples	q_{ij}^W	$q_i^W = \sum_j q_{ij}^W$	$q^W = \frac{1}{2} \sum_{i,j} q_{ij}^W$			
Head quadruples	q_{ij}^H	$q_i^H = \sum_j q_{ij}^H$	$q^H = \frac{1}{2} \sum_{i,j} q_{ij}^H$			
Cycles ¹						
Triangles	T_{ij}	$T_i = \frac{1}{2} \sum_j T_{ij}$	$T = \frac{1}{6} \sum_{i,j} T_{ij}$			
Quadrangles (0 chords)	$Q_{ij}^{(0)}$	$Q_i^{(0)} = \frac{1}{2} \sum_j Q_{ij}^{(0)}$	$Q^{(0)} = \frac{1}{8} \sum_{i,j} Q_{ij}^{(0)}$			
Quadrangles (1 chord)	$Q_{ij}^{(1)}$	$Q_i^{(1)} = \frac{1}{2} \sum_j Q_{ij}^{(1)}$	$Q^{(1)} = \frac{1}{8} \sum_{i,j} Q_{ij}^{(1)}$			
Quadrangles (2 chords)	$Q_{ij}^{(2)}$	$Q_i^{(2)} = \frac{1}{2} \sum_j Q_{ij}^{(2)}$	$Q^{(2)} = \frac{1}{8} \sum_{i,j} Q_{ij}^{(2)}$			
Structural coefficient ²						
Similarity	s_{ij}	$s_i (s_i^W, s_i^H)$	s			
Complementarity	c_{ij}	$c_i (c_i^W, c_i^H)$	c			
Weak complementarity	h_{ij}	$h_i (h_i^W, h_i^H)$	h			

¹ Weighted cycles are counted separately for wedge and head triples/quadruples but according to the same rules. They are denoted by superscripts W or H correspondingly. For instance, T_i^W and T_i^H are weighted triangle counts for a node i based on weights induced by their underlying wedge and head triples.

² Weighted coefficients are marked with hat, e.g. \hat{s}_i denotes weighted node-wise similarity.

4.2. pathcensus package

We implemented all the methods and algorithms for calculating structural coefficients as well as several other utilities including most appropriate null models and auxiliary methods for conducting statistical inference in **pathcensus** package for Python. The core routines are just-in-time compiled to highly optimized C code using *Numba* library [29] ensuring high efficiency. The package has an

extensive documentation including several usage examples. It will be distributed through *Python Package Index* upon publication.

4.3. Network datasets

All network datasets used in this paper were obtained from Netzschleuder network catalogue and repository [38]. In all analyses only largest connected components were used and networks were simplified by removing multilinks and self-loops. Individual network datasets are described below and their unique names within the repository are provided in the following subsection headings. Each dataset can be accessed via a generic link of the form: `networks.skewed.de/net/<name>` where `<name>` is a placeholder which should be substituted with the name of a specific dataset.

Main descriptive statistics for the network datasets are listed in corresponding tables in Supplementary Materials (SM).

4.3.1. Ugandan village networks (`ugandan_village`)

The dataset consists of unweighted and undirected networks of friendship and health advice relations between households in 17 rural villages bordering Lake Victoria in Mayuge District, Uganda. It has been collected and originally studied by Chami et al. [13]. Relations were measured using the name generator approach in which a representative of each household was asked to indicate up to 10 persons considered friends or trustworthy in regard to health issues. Resulting ties were symmetrized. Basic descriptive statistics for the networks are presented in Tab. S3.

4.3.2. Facebook ego-networks sample (`ego_social`)

The dataset consists of 10 ego-network samples from Facebook and a corresponding combined network [33]. The networks are undirected and unweighted. Basic descriptive statistics for the networks are presented in Tab. S4

4.3.3. *C. elegans* interactomes (`celegans_interactomes`)

The dataset consists of 10 networks of protein-protein interaction in *Caenorhabditis elegans* (a very simple and well-studied type of nematode) measured based on different data sources and using different methods [41]. The networks are undirected and unweighted. Basic descriptive statistics for the networks are presented in Tab. S5.

4.3.4. Software dependencies (`software_dependencies`)

The dataset consists of 17 dependency networks for various programming languages/software projects [44, 45, 46]. The original networks are unweighted and directed but for the purpose of our analysis we used their undirected counterparts. Basic descriptive statistics for the networks are presented in Tab. S6.

4.3.5. Jazz collaborations (`jazz_collab`)

This is an undirected and unweighted network ($n = 198$, $m = 2742$) of collaborations between jazz musicians and bands performing between 1912 and 1940 [19]. Basic descriptive statistics for the networks are presented in SM (Tab. S7).

4.3.6. Joshi-Tope human protein interactome (reactome)

A network of human proteins and their binding interactions, extracted from Reactome project ($n = 6327$, $m = 147547$). Nodes represent proteins and an edge represents a binding interaction between two proteins [24]. Basic descriptive statistics for the networks are presented in Tab. S7.

4.3.7. Internet at the level of Autonomous System (internet_as)

A symmetrized snapshot of the structure of the Internet at the level of Autonomous Systems (AS), reconstructed from BGP tables posted by the University of Oregon Route Views Project ($n = 22936$, $m = 48436$). This snapshot was created on 22 July 2006 [25]. Basic descriptive statistics for the networks are presented in Tab. S7.

4.3.8. Character co-appearances in *A Storm of Swords* (game_thrones)

Network of co-appearances of characters in the Game of Thrones series, by George R. R. Martin, and in particular co-appearances in the book *A Storm of Swords* [7]. Nodes are unique characters, and edges are weighted by the number of times two characters appeared within 15 words of each other in the text. Basic descriptive statistics for the networks are presented in Tab. S7.

4.4. Null models and distributions

Observed values of the structural coefficients were calibrated and/or their significance assessed based on two different null models depending on whether a network was weighted or unweighted.

In both cases the chosen null models are members of the general family of Exponential Random Graph Models (ERGM) which can be used to sample networks (of a given size) from a maximum entropy distribution with constraints imposed on expected values of some properties, e.g. degree sequence. Such models can be used to generate randomized replicates of an observed network which condition on a set of selected properties while being maximally unbiased with respect to any other property [42].

Crucially, ERGMs are fully specified by a corresponding set of *sufficient statistics* [31]. For instance, in undirected and unweighted configuration models the target degree sequence is the sufficient statistic fully determining the maximum entropy distribution over networks with n nodes. Therefore, we simulated null distributions of various graph statistics of interest by sampling R times from an appropriate ERGM and then grouping obtained results by unique combinations of sufficient statistics (e.g. unique node degree for node-wise and degree pairs for edge-wise statistics in undirected and unweighted networks) since nodes/edges with the same values of the sufficient statistics are indistinguishable from the vantage point of the model. Then, observed values for any node or edge could be compared against an appropriate null distribution based on values of its sufficient statistic(s).

4.4.1. Undirected Binary Configuration Model

For undirected and unweighted networks we used Undirected Binary Configuration Model (UBCM) [48]. This is an ERGM which samples from a maximum entropy distribution over all networks of a given size constrained to have a specific expected degree sequence.

4.4.2. Undirected Enhanced Configuration Model

For the weighted network of co-appearances (see Sec. 4.3.8) we used Undirected Enhanced Configuration Model (UECM) [48]. This is an ERGM which samples from a maximum entropy distribution over all networks of a given size constrained to have specific expected degree and strength sequences, while assuming that edge weights are positive integers.

4.5. Assessing significance of structural coefficients

Significance of structural coefficients was assessed by comparing observed values of graph-, node- or edge-wise statistics against a simulated null distribution based on R samples from an appropriate configuration model. More concretely, we first group null model samples corresponding to different units of observation (i.e. nodes or edges) by unique combinations of values of their sufficient statistics (e.g. degrees and strengths). Then, we compare each observed value with the distribution of null model values corresponding to nodes/edges with the same sufficient statistics and calculate p -value as the fraction of the distribution greater than or equal to the observed value. Last but not least, the rate of type I error can be controlled using Benjamini-Hochberg False Discovery Rate (FDR) correction [6] or other similar methods.

The above strategy works well out-of-the-box for node-wise coefficients as each node in a null model sample corresponds to a specific node with specific values of sufficient statistics from the observed network. However, in the case of edge-wise coefficients some edges in randomized networks may not correspond to any edge in the observed network. Such observations will be grouped in buckets that will not correspond to any observed combination of sufficient statistics and as such they will be lost from the vantage point of the estimation of p -values. As a result a very large number of null model samples may be required to ensure enough data points per each unique combination of sufficient statistics.

Probably the best way to address this problem is to use estimated model parameters to derive null distributions of graph statistics of interest analytically. However, for many cases of interest, including complementarity coefficients, this is a hard problem which is outside of the scope of this paper. This is why in Sec. 2.8 we used a different approach and estimated p -values in coarse-grained classes by grouping values of sufficient statistics in buckets with sizes growing logarithmically (with base 2). For instance, observations with degree 1 corresponded to one class, observations with degrees 2 and 3 to another, those with degrees between 4 and 7 to yet another class and so on. This way the calculated p -values are only rough approximations, but on the other hand they can be numerically estimated without running extensive computations, even for edge-wise coefficients in models with multiple sufficient statistics per node such as UECM.

5. Acknowledgments

We thank B. Klein and I. Voitalov for an inspiring conversation on complementarity-driven relations few years ago and V. Murcia for a discussion of complementarity in biological systems. We also thank M. Talaga for proofreading and M. Biesaga for help with testing the code.

5.1. Funding

This work was supported by a grant from Polish National Science Center (*Outline of a network-geometric theory of social structure*, 2020/37/N/HS6/00796).

5.2. Author contributions

S.T. and A.N. conceptualized the project. S.T. formulated the mathematical formalism and wrote the related proofs, designed the algorithms and developed their Python implementation in the form of `pathcensus` package. S.T. conducted the data analyses and prepared the figures. S.T. and A.N. wrote the main text together.

5.3. Competing interests

The authors declare no competing interests.

5.4. Data and materials availability

Data and code needed for reproducing the analyses presented in the paper will be made freely available as a *Github* repository and `pathcensus` package will be released at *Python Package Index* upon publication.

References

- [1] Nesreen K. Ahmed, Jennifer Neville, Ryan A. Rossi, and Nick Duffield. 2015. Efficient Graphlet Counting for Large Networks. In *2015 IEEE International Conference on Data Mining*. IEEE, Atlantic City, NJ, USA, 1–10. <https://doi.org/10.1109/ICDM.2015.141>
- [2] Luca Maria Aiello, Alain Barrat, Rossano Schifanella, Ciro Cattuto, Benjamin Markines, and Filippo Menczer. 2012. Friendship Prediction and Homophily in Social Media. *ACM Transactions on the Web* 6, 2 (2012), 1–33. <https://doi.org/10.1145/2180861.2180866>
- [3] Emanuele Aliverti and Daniele Durante. 2019. Spatial Modeling of Brain Connectivity Data via Latent Distance Models with Nodes Clustering. *Statistical Analysis and Data Mining: The ASA Data Science Journal* 12, 3 (2019), 185–196. <https://doi.org/10.1002/sam.11412>
- [4] Delia Baldassarri and Peter Bearman. 2007. Dynamics of Political Polarization. *American Sociological Review* 72, 5 (2007), 784–811. <https://doi.org/10.1177/000312240707200507>
- [5] A. Barrat, M. Barthelemy, R. Pastor-Satorras, and A. Vespignani. 2004. The Architecture of Complex Weighted Networks. *Proceedings of the National Academy of Sciences* 101, 11 (2004), 3747–3752. <https://doi.org/10.1073/pnas.0400087101>
- [6] Yoav Benjamini and Yosef Hochberg. 1995. Controlling the False Discovery Rate: A Practical and Powerful Approach to Multiple Testing. *Journal of the Royal Statistical Society: Series B (Methodological)* 57, 1 (1995), 289–300. <https://doi.org/10.1111/j.2517-6161.1995.tb02031.x>

[7] Andrew Beveridge and Jie Shan. 2016. Network of Thrones. *Math Horizons* 23, 4 (2016), 18–22. <https://doi.org/10.4169/mathhorizons.23.4.18>

[8] Marián Boguñá, Ivan Bonamassa, Manlio De Domenico, Shlomo Havlin, Dmitri Krioukov, and M. Ángeles Serrano. 2021. Network Geometry. *Nature Reviews Physics* 3, 2 (2021), 114–135. <https://doi.org/10.1038/s42254-020-00264-4>

[9] Marián Boguñá, Dmitri Krioukov, Pedro Almagro, and M. Ángeles Serrano. 2020. Small Worlds and Clustering in Spatial Networks. *Physical Review Research* 2, 2 (2020). <https://doi.org/10.1103/PhysRevResearch.2.023040>

[10] Marián Boguñá, Fragkiskos Papadopoulos, and Dmitri Krioukov. 2010. Sustaining the Internet with Hyperbolic Mapping. *Nature Communications* 1, 1 (2010), 62. <https://doi.org/10.1038/ncomms1063>

[11] Marián Boguñá, Romualdo Pastor-Satorras, Albert Díaz-Guilera, and Alex Arenas. 2004. Models of Social Networks Based on Social Distance Attachment. *Physical Review E* 70, 5 (2004), 056122. <https://doi.org/10.1103/PhysRevE.70.056122>

[12] Yann Bramoullé. 2001. Complementarity and Social Networks. *SSRN Electronic Journal* (2001). <https://doi.org/10.2139/ssrn.1028335>

[13] Goylette F. Chami, Sebastian E. Ahnert, Narcis B. Kabatereine, and Edridah M. Tukahewwa. 2017. Social Network Fragmentation and Community Health. *Proceedings of the National Academy of Sciences* 114, 36 (2017), E7425–E7431. <https://doi.org/10.1073/pnas.1700166114>

[14] Seungwha Chung, Harbir Singh, and Kyungmook Lee. 2000. Complementarity, Status Similarity and Social Capital as Drivers of Alliance Formation. *Strategic Management Journal* 21 (2000), 1–22. [https://doi.org/10.1002/\(SICI\)1097-0266\(200001\)21:1<1::AID-SMJ63>3.0.CO;2-P](https://doi.org/10.1002/(SICI)1097-0266(200001)21:1<1::AID-SMJ63>3.0.CO;2-P)

[15] Jesper Dall and Michael Christensen. 2002. Random Geometric Graphs. *Physical Review E* 66, 1 (2002). <https://doi.org/10.1103/PhysRevE.66.016121>

[16] James A. Davis. 1967. Clustering and Structural Balance in Graphs. *Human Relations* 20, 2 (1967), 181–187. <https://doi.org/10.1177/001872676702000206>

[17] Paul Erdős and Alfred Rényi. 1959. On Random Graphs I. *Publicationes Mathematicae* 6 (1959), 290–297.

[18] Thomas Gessey-Jones, Colm Connaughton, Robin Dunbar, Ralph Kenna, Pádraig MacCarron, Cathal O’Conchobhair, and Joseph Yose. 2020. Narrative Structure of *A Song of Ice and Fire* Creates a Fictional World with Realistic Measures of Social Complexity. *Proceedings of the National Academy of Sciences* 117, 46 (2020), 28582–28588. <https://doi.org/10.1073/pnas.2006465117>

[19] Pablo M. Gleiser and Leon Danon. 2003. Community Structure in Jazz. *Advances in Complex Systems* 06, 04 (2003), 565–573. <https://doi.org/10.1142/S0219525903001067>

[20] Harrison Hartle, Brennan Klein, Stefan McCabe, Alexander Daniels, Guillaume St-Onge, Charles Murphy, and Laurent Hébert-Dufresne. 2020. Network Comparison and the Within-Ensemble Graph Distance. *Proceedings of the Royal Society A: Mathematical, Physical and Engineering Sciences* 476, 2243 (2020), 20190744. <https://doi.org/10.1098/rspa.2019.0744>

[21] Trevor Hastie, Robert Tibshirani, and Jerome Friedman. 2008. *The Elements of Statistical Learning* (second ed.). Springer.

[22] Desmond J. Higham, Marija Rašajski, and Nataša Pržulj. 2008. Fitting a Geometric Graph to a Protein–Protein Interaction Network. *Bioinformatics* 24, 8 (2008), 1093–1099. <https://doi.org/10.1093/bioinformatics/btn079>

[23] Mingshan Jia, Bogdan Gabrys, and Katarzyna Musial. 2020. Measuring Quadrangle Formation in Complex Networks. *arXiv:2011.10763 [cs]* (2020). arXiv:cs/2011.10763

[24] G. Joshi-Tope. 2004. Reactome: A Knowledgebase of Biological Pathways. *Nucleic Acids Research* 33, Database issue (2004), D428–D432. <https://doi.org/10.1093/nar/gki072>

[25] Brian Karrer, M. E. J. Newman, and Lenka Zdeborová. 2014. Percolation on Sparse Networks. *Physical Review Letters* 113, 20 (2014), 208702. <https://doi.org/10.1103/PhysRevLett.113.208702>

[26] Maksim Kitsak. 2020. Latent Geometry for Complementarity-Driven Networks. *arXiv:2003.06665 [cond-mat, physics:physics]* (2020). arXiv:cond-mat, physics:physics/2003.06665

[27] Gueorgi Kossinets and D. J. Watts. 2009. Origins of Homophily in an Evolving Social Network. *Amer. J. Sociology* 115, 2 (2009), 405–450. <https://doi.org/10.1086/599247>

[28] Dmitri Krioukov. 2016. Clustering Implies Geometry in Networks. *Physical Review Letters* 116, 20 (2016). <https://doi.org/10.1103/PhysRevLett.116.208302>

[29] Siu Kwan Lam, Antoine Pitrou, and Stanley Seibert. 2015. Numba: A LLVM-based Python JIT Compiler. In *Proceedings of the Second Workshop on the LLVM Compiler Infrastructure in HPC - LLVM '15*. ACM Press, Austin, Texas, 1–6. <https://doi.org/10.1145/2833157.2833162>

[30] Michael C. Lawrence and Peter M. Colman. 1993. Shape Complementarity at Protein/Protein Interfaces. *Journal of Molecular Biology* 234, 4 (1993), 946–950. <https://doi.org/10.1006/jmbi.1993.1648>

[31] E. L. Lehmann and George Casella. 1998. *Theory of Point Estimation* (2nd ed ed.). Springer, New York.

[32] Peter V. Marsden. 1988. Homogeneity in Confiding Relations. *Social Networks* 10, 1 (1988), 57–76. [https://doi.org/10.1016/0378-8733\(88\)90010-X](https://doi.org/10.1016/0378-8733(88)90010-X)

[33] Julian McAuley and Jure Leskovec. 2012. Learning to Discover Social Circles in Ego Networks. In *Advances in Neural Information Processing Systems*, Vol. 25. Curran Associates, Inc.

[34] J. M. McPherson, L. Smith-Lovin, and J. M. Cook. 2001. Birds of a Feather: Homophily in Social Networks. *Annual Review of Sociology* 27, 1 (2001), 415–444. <https://doi.org/10.1146/annurev.soc.27.1.415>

[35] R. Milo. 2002. Network Motifs: Simple Building Blocks of Complex Networks. *Science* 298, 5594 (2002), 824–827. <https://doi.org/10.1126/science.298.5594.824>

[36] M. E. J. Newman. 2010. *Networks: An Introduction*. Oxford University Press, Oxford, New York.

[37] Tiago P. Peixoto. 2017. Nonparametric Bayesian Inference of the Microcanonical Stochastic Block Model. *Physical Review E* 95, 1 (2017), 012317. <https://doi.org/10.1103/PhysRevE.95.012317>

[38] Tiago P. Peixoto. 2020. The Netzschleuder Network Catalogue and Repository. <https://networks.skewed.de/>.

[39] Tiago P. Peixoto. 2021. Descriptive vs. Inferential Community Detection: Pitfalls, Myths and Half-Truths. *arXiv:2112.00183 [physics, stat]* (2021). arXiv:physics, stat/2112.00183

[40] Tuan M. Pham, Andrew C. Alexander, Jan Korbel, Rudolf Hanel, and Stefan Thurner. 2021. Balance and Fragmentation in Societies with Homophily and Social Balance. *Scientific Reports* 11, 1 (2021), 17188. <https://doi.org/10.1038/s41598-021-96065-5>

[41] Nicolas Simonis, Jean-François Rual, Anne-Ruxandra Carvunis, Murat Tasan, Irma Lemmens, Tomoko Hirozane-Kishikawa, Tong Hao, Julie M Sahalie, Kavitha Venkatesan, Fana Gebreab, Sebiha Cevik, Niels Klitgord, Changyu Fan, Pascal Braun, Ning Li, Nono Ayivi-Guedehoussou, Elizabeth Dann, Nicolas Bertin, David Szeto, Amélie Dricot, Muhammed A Yildirim, Chenwei Lin, Anne-Sophie de Smet, Huey-Ling Kao, Christophe Simon, Alex Smolyar, Jin Sook Ahn, Muneesh Tewari, Mike Boxem, Stuart Milstein, Haiyuan Yu, Matija Dreze, Jean Vandenhautte, Kristin C Gunsalus, Michael E Cusick, David E Hill, Jan Tavernier, Frederick P Roth, and Marc Vidal. 2009. Empirically Controlled Mapping of the *Caenorhabditis Elegans* Protein-Protein Interactome Network. *Nature Methods* 6, 1 (2009), 47–54. <https://doi.org/10.1038/nmeth.1279>

[42] Tiziano Squartini, Rossana Mastrandrea, and Diego Garlaschelli. 2015. Unbiased Sampling of Network Ensembles. *New Journal of Physics* 17, 2 (2015), 023052. <https://doi.org/10.1088/1367-2630/17/2/023052>

[43] Pulipati Srilatha and Ramakrishnan Manjula. 2016. Similarity Index Based Link Prediction Algorithms in Social Networks: A Survey. *Journal of Telecommunications and Information Technology* 2 (2016), 87–94.

[44] Lovro Šubelj and Marko Bajec. 2011. Community Structure of Complex Software Systems: Analysis and Applications. *Physica A: Statistical Mechanics and its Applications* 390, 16 (2011), 2968–2975. <https://doi.org/10.1016/j.physa.2011.03.036>

[45] Lovro Šubelj and Marko Bajec. 2012. Software Systems through Complex Networks Science: Review, Analysis and Applications. In *Proceedings of the First International Workshop on Software Mining*. 9–16. <https://doi.org/10.1145/2384416.2384418>

[46] Lovro Šubelj, Slavko Žitnik, Neli Blagus, and Marko Bajec. 2014. Node Mixing and Group Structure of Complex Software Networks. *Advances in Complex Systems* 17, 07n08 (2014), 1450022. <https://doi.org/10.1142/S0219525914500222>

[47] Szymon Talaga and Andrzej Nowak. 2020. Homophily as a Process Generating Social Networks: Insights from Social Distance Attachment Model. *Journal of Artificial Societies and Social Simulation* 23, 2 (2020), 6. <https://doi.org/10.18564/jasss.4252>

[48] Nicolò Vallarano, Matteo Bruno, Emiliano Marchese, Giuseppe Trapani, Fabio Saracco, Giulio Cimini, Mario Zanon, and Tiziano Squartini. 2021. Fast and Scalable Likelihood Maximization for Exponential Random Graph Models with Local Constraints. *Scientific Reports* 11, 1 (2021), 15227. <https://doi.org/10.1038/s41598-021-93830-4>

[49] Remco van der Hofstad, Johan S. H. van Leeuwaarden, and Clara Stegehuis. 2018. Triadic Closure in Configuration Models with Unbounded Degree Fluctuations. *Journal of Statistical Physics* 173, 3-4 (2018), 746–774. <https://doi.org/10.1007/s10955-018-1952-x>

[50] Nguyen Xuan Vinh, Julien Epps, and James Bailey. 2010. Information Theoretic Measures for Clusterings Comparison: Variants, Properties, Normalization and Correction for Chance. *The Journal of Machine Learning Research* 11 (2010), 2837–2854.

[51] Stanley Wasserman and Katherine Faust. 1994. *Social Network Analysis: Methods and Applications*. Cambridge University Press, Cambridge; New York.

[52] D. J. Watts and S. H. Strogatz. 1998. Collective Dynamics of ‘Small-World’ Networks. *Nature* 393, 6684 (1998), 440. <https://doi.org/10.1038/30918>

[53] Wen-Jie Xie, Ming-Xia Li, Zhi-Qiang Jiang, Qun-Zhao Tan, Boris Podobnik, Wei-Xing Zhou, and H. Eugene Stanley. 2016. Skill Complementarity Enhances Heterophily in Collaboration Networks. *Scientific Reports* 6, 1 (2016). <https://doi.org/10.1038/srep18727>

[54] Hao Yin, Austin R. Benson, and Jure Leskovec. 2019. The Local Closure Coefficient: A New Perspective On Network Clustering. In *Proceedings of the Twelfth ACM International Conference on Web Search and Data Mining*. ACM, Melbourne VIC Australia, 303–311. <https://doi.org/10.1145/3289600.3290991>

[55] Peng Zhang, Jinliang Wang, Xiaojia Li, Menghui Li, Zengru Di, and Ying Fan. 2008. Clustering Coefficient and Community Structure of Bipartite Networks. *Physica A: Statistical Mechanics and its Applications* 387, 27 (2008), 6869–6875. <https://doi.org/10.1016/j.physa.2008.09.006>

Supplementary Materials

S1. Similarity and structural equivalence

Here we derive the relationship between nodal similarity coefficient s_i and structural equivalence between a node i and its neighbors. First, we show that s_i is a weighted average of node-wise coefficients s_{ij} 's for $j \in \mathcal{N}_1(i)$, that is:

$$s_i = \frac{4T_i}{t_i^W + t_i^H} = \frac{\sum_j (t_{ij}^W + t_{ij}^H) s_{ij}}{\sum_j t_{ij}^W + t_{ij}^H} \quad (\text{S1})$$

Note that Eq. (4) implies that $(t_{ij}^W + t_{ij}^H) s_{ij} = 2T_{ij}$. Moreover, since each triangle including i is shared with two other nodes we have that:

$$\sum_{j \in \mathcal{N}_1(i)} (t_{ij}^W + t_{ij}^H) s_{ij} = \sum_{j \in \mathcal{N}_1(i)} 2T_{ij} = 4T_i \quad (\text{S2})$$

On the other hand, $t_{ij}^W + t_{ij}^H$ is the number of 2-paths traversing the (i, j) edges so it can be written as $t_{ij}^W + t_{ij}^H = d_i + d_j - 2$. Hence, it is easy to see that:

$$\begin{aligned} \sum_{j \in \mathcal{N}_1(i)} t_{ij}^W + t_{ij}^H &= \sum_{j \in \mathcal{N}_1(i)} (d_i + d_j - 2) \\ &= d_i(d_i - 1) + \sum_{j \in \mathcal{N}_1(i)} (d_j - 1) \\ &= t_i^W + t_i^H \end{aligned} \quad (\text{S3})$$

Finally, substituting (S2) and (S3) into (S1) we confirm the desired equality.

Now, following Eq. (7.55) in [36] we note the relationship between Sørensen Index (normalized Hamming similarity) for connected nodes i and j and s_{ij} (4):

$$H_{ij} = \frac{2T_{ij}}{d_i + d_j} = s_{ij} \frac{d_i + d_j - 2}{d_i + d_j} \quad (\text{S4})$$

Note that the above implies that $H_{ij} < s_{ij}$ for all (i, j) edges for which s_{ij} is defined. And since we established that s_i is a weighted average of s_{ij} 's with $j \in \mathcal{N}_1(i)$ we have that:

$$\min_j H_{ij} < \min_j s_{ij} \leq s_i \leq \max_j s_{ij} = \max_j \left(H_{ij} \frac{d_i + d_j}{d_i + d_j - 2} \right) \quad (\text{S5})$$

which proves inequality (5). Note that for large values of $d_i + d_j$ the above is approximately equivalent to:

$$\min_j H_{ij} < s_i \leq \max_j H_{ij} \quad (\text{S6})$$

In other words, we showed that the similarity coefficient of a node i is approximately bounded between minimum and maximum structural equivalence (Sørensen Index) between itself and any of its neighbors.

S2. Complementarity and structural equivalence

Here we derive the relationship between nodal complementarity coefficient c_i and structural equivalence. We start by showing that c_i is a weighted average of edge-wise coefficients c_{ij} 's for $j \in \mathcal{N}_1(i)$, that is:

$$c_i = \frac{4Q_{ij}}{q_i^W + q_i^H} = \frac{\sum_j (q_{ij}^W + q_{ij}^H) c_{ij}}{\sum_j q_{ij}^W + q_{ij}^H} \quad (\text{S7})$$

Using Eq. (10) we can write $2Q_{ij} = (q_{ij}^W + q_{ij}^H) c_{ij}$. Moreover, each quadrangle including a node i is shared with exactly two other nodes. Hence, we have that:

$$\sum_{j \in \mathcal{N}_1} (q_{ij}^W + q_{ij}^H) c_{ij} = \sum_{j \in \mathcal{N}_1(i)} 2Q_{ij} = 4Q_i \quad (\text{S8})$$

Next, note that each 3-path starting at an (i, j) edge defines a unique ordered quadruple of the form (i, j, k, l) or (j, i, k, l) . The first form is counted as a head quadruple of the node i and a wedge quadruple of the node j and in the second case the order is reversed. And since $q_{ij}^W + q_{ij}^H$ is the number of 3-paths starting at the (i, j) edge it must hold that the:

$$\sum_{j \in \mathcal{N}_1(i)} q_{ij}^W + q_{ij}^H = q_i^W + q_i^H \quad (\text{S9})$$

Finally, note that (S8) and (S9) jointly mean that Eq. (S7) must be true. As a result, for $j \in \mathcal{N}_1(i)$ we have that:

$$\min_j c_{ij} \leq c_i \leq \max_j c_{ij} \quad (\text{S10})$$

Now, in order to derive the connection between complementarity coefficients and structural equivalence we need to use weak complementarity introduced in Sec. 2.3. Thus, first we focus on finding bounds for h_{ij} which is a much easier task.

Let $Q_{ij}^{(0,1,2)} = Q_{ij}^{(0)} + Q_{ij}^{(1)} + Q_{ij}^{(2)}$ be the number of quadrangles with any number of chords incident to the (i, j) edge. It is easy to see that:

$$Q_{ij}^{(0,1,2)} = \sum_{k \in \mathcal{N}_1(i) - \{j\}} n_{jk} - 1 \quad (\text{S11})$$

On the other hand, the number of 3-paths starting at the (i, j) edge is:

$$\begin{aligned} q_{ij}^W + q_{ij}^H &= \sum_{k \in \mathcal{N}_1(i) - \{j\}} (d_k - 1) + \sum_{l \in \mathcal{N}_1(j) - \{i\}} (d_l - 1) - 2n_{ij} \\ &= \sum_{k \in \mathcal{N}_1(i) - \{j\}} (d_k - 1 - a_{jk}) + \sum_{l \in \mathcal{N}_1(j) - \{i\}} (d_l - 1 - a_{il}) \end{aligned} \quad (\text{S12})$$

since q_{ij}^W is the number of (j, i, k, l) and q_{ij}^H of (i, j, k, l) quadruples. The second equality comes from the fact that $n_{ij} = \sum_k a_{jk} = \sum_l a_{il}$. Now, we can use the two above results and the Asymmetric Excess Sørensen Index defined in Eq. (11) to rewrite the weak edge-wise complementarity as:

$$h_{ij} = \frac{\sum_k (d_k - 1 - a_{jk}) H_{kj|i} + \sum_l (d_l - 1 - a_{il}) H_{li|j}}{\sum_k (d_k - 1 - a_{jk}) + \sum_l (d_l - 1 - a_{il})} \quad (\text{S13})$$

As a result we have that:

$$\min_{k,l}(H_{kj|i}, H_{li|j}) \leq h_{ij} \leq \max_{k,l}(H_{kj|i}, H_{li|j}) \quad (\text{S14})$$

Using Eq. (S10) we can write:

$$\min_{j,k,l}(H_{kj|i}, H_{li|j}) \leq h_i \leq \max_{j,k,l}(H_{kj|i}, H_{li|j}) \quad (\text{S15})$$

Finally, since by definition $c_{ij} \leq h_{ij}$ this proves Eq. (12). In other words, we just showed that structural complementarity coefficient defined for a node i is bounded from above by the maximum Asymmetric Excess Sørenson Index between any two of its neighbors or itself and any neighbor of its neighbors. Intuitively, high complementarity can exist only in the presence of high structural equivalence between neighbors of i as well as i and neighbors of its neighbors. Moreover, in the weak case we also have a lower bound of the same nature.

S3. PathCensus and structural coefficients

S3.1. Unweighted version

Algorithm S1 Unweighted PathCensus algorithm. It takes an undirected graph $G = (V, E)$ with $|V| = n$ and $|E| = m$ as input and returns edge-wise counts of wedge and head triples and quadruples, triangles as well as strong and weak quadrangles.

```

1: Initialize empty  $C$                                  $\triangleright m \times 8$  array for storing path counts
2: Initialize  $R$  such that  $R_i = 0 \quad \forall i \in V$        $\triangleright n \times 1$  array for keeping track of node roles
3: Let  $D$  be the degree sequence of  $G$                    $\triangleright n \times 1$  array
4: Initialize  $u = 0$ 
5: for  $e = (i, j) \in E$  do                                 $\triangleright$  the loop may be parallelized
6:   Set  $u = u + 1$ 
7:   Initialize  $T_{ij}, t_{ij}^W, t_{ij}^H = 0$                    $\triangleright$  counts of triangles and wedge and head triples
8:   Initialize  $Q_{ij}^{(0)}, Q_{ij}^{(1)}, Q_{ij}^{(2)} = 0$        $\triangleright$  counts of quadrangles with 0, 1 and 2 chordal edges
9:   Initialize  $q_{ij}^W, q_{ij}^H = 0$                        $\triangleright$  counts of wedge and head quadruples
10:  Initialize  $\text{Star}_i, \text{Star}_j, \text{Tri}_{ij} = \emptyset$      $\triangleright$  Empty sets for keeping track of nodes with different roles
11:  for  $(k \neq j) \in \mathcal{N}_1(i)$  do
12:    Add  $k$  to  $\text{Star}_i$  and set  $R_k = 1$ 
13:    Set  $t_{ij}^W = t_{ij}^W + 1$ 
14:  for  $(k \neq i) \in \mathcal{N}_1(j)$  do
15:    if  $R_k = 1$  then
16:       $T_{ij} = T_{ij} + 1$ 
17:      Remove  $k$  from  $\text{Star}_i$  and set  $R_k = 3$ 
18:    else
19:      Add  $k$  to  $\text{Star}_j$  and set  $R_k = 2$ 
20:       $t_{ij}^H = t_{ij}^H + 1$ 
21:  for  $(k \neq j) \in \mathcal{N}_1(i)$  do                   $\triangleright$  This internal nested loop determines computational complexity
22:    for  $(l \neq i, j)$  do
23:       $q_{ij}^W = q_{ij}^W + 1$ 
24:      if  $R_k = 1 \vee R_l = 2$  then
25:         $Q_{ij}^{(0)} = Q_{ij}^{(0)} + 1$ 
26:      else if  $(R_k = 3 \wedge R_l = 2) \vee (R_k = 1 \wedge R_l = 3)$  then
27:         $Q_{ij}^{(1)} = Q_{ij}^{(1)} + 1$ 
28:      else if  $R_k = 3 \wedge R_l = 3$  then
29:         $Q_{ij}^{(2)} = Q_{ij}^{(2)} + 1$ 
30:  for  $k \in \text{Star}_i$  do
31:    Set  $R_k = 0$ 
32:  for  $k \in \text{Star}_j$  do
33:    Set  $q_{ij}^H = q_{ij}^H + D_k - 1$  and set  $R_k = 0$ 
34:  for  $k \in \text{Tri}_{ij}$  do
35:    Set  $q_{ij}^H = q_{ij}^H + D_k - 2$  and set  $R_k = 0$ 
36:  Set  $C_u = (T_{ij}, t_{ij}^W, t_{ij}^H, Q_{ij}^{(0)}, Q_{ij}^{(1)}, Q_{ij}^{(2)}, q_{ij}^W, q_{ij}^H)$        $\triangleright$  Set  $u$ -th row of  $C$ 
37: return  $C$ 

```

S3.2. Weighted version

Algorithm S2 Weighted PathCensus algorithm. It takes an undirected weighted graph $G = (V, E)$ with $|V| = n$, $|E| = m$ and weights w_{ij} for $(i, j) \in E$ as input and returns edge-wise weighted counts of wedge and head triples and quadruples, triangles as well as strong and weak quadrangles.

```

1: Initialize empty  $C$                                  $\triangleright m \times 12$  array for storing path counts
2: Initialize  $R$  such that  $R_i = 0 \quad \forall i \in V$      $\triangleright n \times 1$  array for keeping track of node roles
3: Let  $D$  be the degree sequence of  $G$                  $\triangleright n \times 1$  array
4: Let  $S$  be the strength sequence of  $G$                $\triangleright n \times 1$  array
5: Let  $W$  be a map from edges  $(i, j) \in E$  to weights  $w_{ij}$ 
6: Initialize  $u = 0$ 
7: for  $e = (i, j) \in E$  do                                 $\triangleright$  the loop may be parallelized
8:   Set  $u = u + 1$ 
9:   Initialize  $T_{ij}^W, T_{ij}^H, t_{ij}^W, t_{ij}^H = 0$            $\triangleright$  counts of wedge/head triangles and triples
10:  Initialize  $Q_{ij}^{W(0)}, Q_{ij}^{W(1)}, Q_{ij}^{W(2)} = 0$        $\triangleright$  counts of wedge quadrangles with 0/1/2 chordal edges
11:  Initialize  $Q_{ij}^{H(0)}, Q_{ij}^{H(1)}, Q_{ij}^{H(2)} = 0$        $\triangleright$  counts of head quadrangles with 0/1/2 chordal edges
12:  Initialize  $q_{ij}^W, q_{ij}^H = 0$                           $\triangleright$  counts of wedge and head quadruples
13:  Initialize  $\text{Star}_i, \text{Star}_j, \text{Tri}_{ij} = \emptyset$        $\triangleright$  Empty sets for keeping track of nodes with different roles
14:  for  $(k \neq j) \in \mathcal{N}_1(i)$  do
15:    Add  $k$  to  $\text{Star}_i$  and set  $R_k = 1$ 
16:    Set  $t_{ij}^W = t_{ij}^W + (W(i, j) + W(i, k))/2$ 
17:  for  $(k \neq i) \in \mathcal{N}_1(j)$  do
18:    if  $R_k = 1$  then
19:       $T_{ij}^W = T_{ij}^H + (W(i, j) + W(i, k))/2$ 
20:       $T_{ij}^H = T_{ij}^H + (W(i, j) + W(j, k))/2$ 
21:      Remove  $k$  from  $\text{Star}_i$  and set  $R_k = 3$ 
22:    else
23:      Add  $k$  to  $\text{Star}_j$  and set  $R_k = 2$ 
24:       $t_{ij}^H = t_{ij}^H + (W(i, j) + W(j, k))/2$ 
25:  for  $(k \neq j) \in \mathcal{N}_1(i)$  do                                 $\triangleright$  This internal nested loop determines computational complexity
26:    for  $(l \neq i, j)$  do
27:       $q_{ij}^W = q_{ij}^W + (W(i, j) + W(i, k) + W(k, l))/3$ 
28:      if  $R_k = 1 \vee R_l = 2$  then
29:         $Q_{ij}^{W(0)} = Q_{ij}^{W(0)} + (W(i, j) + W(i, k) + W(k, l))/3$ 
30:         $Q_{ij}^{H(0)} = Q_{ij}^{H(0)} + (W(i, j) + W(j, l) + W(k, l))/3$ 
31:      else if  $(R_k = 3 \wedge R_l = 2) \vee (R_k = 1 \wedge R_l = 3)$  then
32:         $Q_{ij}^{W(1)} = Q_{ij}^{W(1)} + (W(i, j) + W(i, k) + W(k, l))/3$ 
33:         $Q_{ij}^{H(1)} = Q_{ij}^{H(1)} + (W(i, j) + W(j, l) + W(k, l))/3$ 
34:      else if  $R_k = 3 \wedge R_l = 3$  then
35:         $Q_{ij}^{W(2)} = Q_{ij}^{W(2)} + (W(i, j) + W(i, k) + W(k, l))/3$ 
36:         $Q_{ij}^{H(2)} = Q_{ij}^{H(2)} + (W(i, j) + W(j, l) + W(k, l))/3$ 
37:  for  $k \in \text{Star}_i$  do Set  $R_k = 0$ 
38:  for  $k \in \text{Star}_j$  do
39:    Set  $q_{ij}^H = q_{ij}^H + [(D_i - 1)(W(i, j) + W(j, k)) + S_k - W(j, k)]/3$  and set  $R_k = 0$ 
40:  for  $k \in \text{Tri}_{ij}$  do
41:    Set  $q_{ij}^H = q_{ij}^H + [(D_i - 2)(W(i, j) + W(j, k)) + S_k - W(j, k) - W(i, k)]/3$  and set  $R_k = 0$ 
42:  Set  $C_u = (T_{ij}^W, T_{ij}^H, t_{ij}^W, t_{ij}^H, Q_{ij}^{W(0)}, Q_{ij}^{H(0)}, Q_{ij}^{W(1)}, Q_{ij}^{H(1)}, Q_{ij}^{W(2)}, Q_{ij}^{H(2)}, q_{ij}^W, q_{ij}^H)$        $\triangleright$  Set  $u$ -th row of  $C$ 
43: return  $C$ 

```

S3.3. Calculating counts for reversed edges

Note that in our implementation t_{ij}^W counts the number of (k, i, j) and t_{ij}^H tracks (i, j, k) triples. Thus, we have that $t_{ij}^W = t_{ji}^H$ and *vice versa*. Similarly, q_{ij}^W counts (j, i, k, l) and q_{ij}^H (i, j, k, l) quadruples, so again we have that $q_{ij}^W = q_{ji}^H$ and *vice versa*. On the other hand, counts of triangles and quadrangles are symmetric. However, in the weighted case wedge and head triangles/quadrangles need to be swapped in the same way as triples and quadruples. As a result, for the purpose of counting we can assume that all edges are of the form $i < j$ and still be able to count everything correctly. In other words there is no need to consider each undirected edge twice.

S3.4. Computational complexity

It is clear from the structure of the three nested loops that the asymptotic worst-case computational complexity of both algorithms is $O(md_{\max}^2)$ where m is the number of edges and d_{\max} is the maximum node degree. This agrees with the analysis presented in Ref. [1]. However, in practice the runtime can be reduced by enforcing that edges are defined to satisfy the condition $d_i \leq d_j$ (note that this can always be done without loss of generality). The impact of this optimization can be quite significant for networks with highly heterogeneous degree distributions. For instance, in the case of the network of Internet at the level of Autonomous System ($n = 22936$; $\langle d_i \rangle = 4.22$; $d_{\max} = 2390$) it yields more than five times shorter computation times on average.

S3.5. Structural coefficients: formulas

Tabs. S1 and S2 below define formulas for all structural coefficients. They are expressed in terms of path and cycle counts defined in Tab. 1.

Table S1. Formulas for unweighted structural coefficients based on path and cycle counts

Relational principle				
Level	Coefficient	Similarity	Complementarity	Weak complementarity
Edges	Structural	$s_{ij} = \frac{2T_{ij}}{t_{ij}^W + t_{ij}^H}$	$c_{ij} = \frac{2Q_{ij}}{q_{ij}^W + q_{ij}^H}$	$h_{ij} = \frac{2(Q_{ij}^{(0)} + Q_{ij}^{(1)} + Q_{ij}^{(2)})}{q_{ij}^W + q_{ij}^H}$
Nodes	Structural	$s_i = \frac{4T_i}{t_i^W + t_i^H}$	$c_i = \frac{4Q_i}{q_i^W + q_i^H}$	$h_i = \frac{4(Q_i^{(0)} + Q_i^{(1)} + Q_i^{(2)})}{q_i^W + q_i^H}$
	Clustering	$s_i^W = \frac{2T_i}{t_i^W}$	$c_i^W = \frac{2Q_i}{q_i^W}$	$h_i^W = \frac{2(Q_i^{(0)} + Q_i^{(1)} + Q_i^{(2)})}{q_i^W}$
	Closure	$s_i^H = \frac{2T_i}{t_i^H}$	$c_i^H = \frac{2Q_i}{q_i^H}$	$h_i^H = \frac{2(Q_i^{(0)} + Q_i^{(1)} + Q_i^{(2)})}{q_i^H}$
Global [†]	Structural	$s = \frac{6T}{t^W + t^H}$	$c = \frac{8Q}{q^W + q^H}$	$h = \frac{8(Q^{(0)} + 8Q^{(1)} + 8Q^{(2)})}{q^W + q^H}$
	Clustering	$s^W = \frac{3T}{t^W}$	$c^W = \frac{4Q}{q^W}$	$h^W = \frac{4(Q^{(0)} + Q^{(1)} + Q^{(2)})}{q^W}$
	Closure	$s^H = \frac{3T}{t^H}$	$c^H = \frac{4Q}{q^H}$	$h^H = \frac{4(Q^{(0)} + Q^{(1)} + Q^{(2)})}{q^W + q^H}$

[†] – All global measures are equivalent.

Table S2. Formulas for weighted structural coefficients based on path and cycle counts

Relational principle				
Level	Coefficient	Similarity	Complementarity	Weak complementarity
Edges	Structural	$\hat{s}_{ij} = \frac{T_{ij}^W + T_{ij}^H}{t_{ij}^W + t_{ij}^H}$	$\hat{c}_{ij} = \frac{Q_{ij}^W + Q_{ij}^H}{q_{ij}^W + q_{ij}^H}$	$\hat{h}_{ij} = \frac{Q_{ij}^{W(0)} + Q_{ij}^{H(0)} + Q_{ij}^{W(1)} + Q_{ij}^{H(1)} + Q_{ij}^{W(2)} + Q_{ij}^{H(2)}}{q_{ij}^W + q_{ij}^H}$
Nodes	Structural	$\hat{s}_i = \frac{2T_i^W + 2T_i^H}{t_i^W + t_i^H}$	$\hat{c}_i = \frac{2Q_i^W + 2Q_i^H}{q_i^W + q_i^H}$	$\hat{h}_i = \frac{2(Q_i^{W(0)} + Q_i^{H(0)} + Q_i^{W(1)} + Q_i^{H(1)} + Q_i^{W(2)} + Q_i^{H(2)})}{q_i^W + q_i^H}$
	Clustering	$\hat{s}_i^W = \frac{2T_i^W}{t_i^W}$	$\hat{c}_i^W = \frac{2Q_i^W}{q_i^W}$	$\hat{h}_i^W = \frac{2(Q_i^{W(0)} + Q_i^{W(1)} + Q_i^{W(2)})}{q_i^W}$
	Closure	$\hat{s}_i^H = \frac{2T_i^H}{t_i^H}$	$\hat{c}_i^H = \frac{2Q_i^H}{q_i^H}$	$\hat{h}_i^H = \frac{2(Q_i^{H(0)} + Q_i^{H(1)} + Q_i^{H(2)})}{q_i^H}$
Global [†]	Structural	$\hat{s} = \frac{3T^W + 3T^H}{t^W + t^H}$	$\hat{c} = \frac{4Q^W + 4Q^H}{q^W + q^H}$	$\hat{h} = \frac{4(Q^{W(0)} + Q^{H(0)} + Q^{W(1)} + Q^{H(1)} + Q^{W(2)} + Q^{H(2)})}{q^W + q^H}$
	Clustering	$\hat{s}^W = \frac{3T^W}{t^W}$	$\hat{c}^W = \frac{4Q^W}{q^W}$	$\hat{h}^W = \frac{4(Q^{W(0)} + Q^{W(1)} + Q^{W(2)})}{q^W}$
	Closure	$\hat{s}^H = \frac{3T^H}{t^H}$	$\hat{c}^H = \frac{4Q^H}{q^H}$	$\hat{h}^H = \frac{4(Q^{H(0)} + Q^{H(1)} + Q^{H(2)})}{q^W + q^H}$

[†] – All global measures are equivalent.

S4. Network datasets: descriptive statistics

Table S3. Descriptive statistics for Ugandan village networks ($N = 34$)

domain	network	s	c	h	n	S	ρ	$\langle d_i \rangle$	σ_{d_i}	d_{\max}
social (offline)	friendship-1	0.06	0.03	0.05	202	1.00	0.03	5.42	0.72	32
	friendship-2	0.11	0.05	0.09	181	0.99	0.04	7.60	0.77	44
	friendship-3	0.13	0.06	0.12	192	1.00	0.06	11.04	0.74	53
	friendship-4	0.09	0.05	0.08	320	1.00	0.04	12.97	0.66	50
	friendship-5	0.12	0.05	0.09	184	1.00	0.04	7.83	0.69	30
	friendship-6	0.14	0.07	0.12	139	1.00	0.07	9.09	0.68	42
	friendship-7	0.17	0.09	0.15	121	1.00	0.11	12.73	0.52	32
	friendship-8	0.06	0.04	0.05	369	1.00	0.03	9.50	0.70	58
	friendship-9	0.16	0.06	0.14	178	1.00	0.07	12.02	0.78	80
	friendship-10	0.10	0.07	0.09	207	1.00	0.05	10.55	0.64	44
	friendship-11	0.09	0.04	0.07	250	1.00	0.03	8.50	0.70	44
	friendship-12	0.08	0.05	0.08	229	1.00	0.03	7.62	0.86	58
	friendship-13	0.10	0.06	0.09	183	1.00	0.05	8.84	0.68	34
	friendship-14	0.15	0.06	0.12	124	1.00	0.07	8.47	0.64	36
	friendship-15	0.07	0.04	0.06	120	1.00	0.04	4.57	0.70	17
	friendship-16	0.05	0.03	0.04	372	1.00	0.02	7.38	0.72	43
	friendship-17	0.25	0.07	0.22	65	1.00	0.12	7.91	0.70	31
	health-advice_1	0.05	0.04	0.10	187	0.98	0.02	4.61	1.31	60
	health-advice_2	0.06	0.06	0.11	170	1.00	0.03	4.64	1.66	70
	health-advice_3	0.08	0.05	0.15	185	1.00	0.04	6.90	1.43	78
	health-advice_4	0.06	0.04	0.06	316	1.00	0.02	6.61	0.96	72
	health-advice_5	0.09	0.02	0.11	166	0.99	0.03	4.65	1.45	70
	health-advice_6	0.06	0.02	0.14	131	0.98	0.03	4.34	1.93	75
	health-advice_7	0.14	0.06	0.14	121	1.00	0.07	7.82	0.80	46
	health-advice_8	0.05	0.03	0.05	361	1.00	0.02	6.85	1.04	84
	health-advice_9	0.10	0.05	0.15	173	1.00	0.04	7.20	1.42	98
	health-advice_10	0.13	0.05	0.14	204	1.00	0.04	8.04	0.98	71
	health-advice_11	0.05	0.04	0.11	234	0.97	0.02	4.50	1.67	85
	health-advice_12	0.04	0.04	0.06	218	0.99	0.02	4.90	1.30	79
	health-advice_13	0.06	0.03	0.07	157	0.91	0.02	3.64	1.25	51
	health-advice_14	0.11	0.05	0.09	120	1.00	0.05	5.43	0.80	26
	health-advice_15	0.06	0.05	0.11	117	1.00	0.03	3.35	1.36	34
	health-advice_16	0.04	0.01	0.13	349	1.00	0.01	4.94	2.21	152
	health-advice_17	0.13	0.06	0.15	63	1.00	0.07	4.63	0.95	28
Average		0.09	0.05	0.10	197.29	0.99	0.04	7.21	1.01	56.09

s - global similarity (clustering)

c - global complementarity

h - global complementarity (weak)

n - number of nodes in the giant component

S - relative size of the giant component

ρ - edge density

$\langle d_i \rangle$ - average node degree

σ_{d_i} - coefficient of variation of node degrees

d_{\max} - maximum node degree

Table S4. Descriptive statistics for Facebook ego networks sample ($N = 11$)

domain	network	<i>s</i>	<i>c</i>	<i>h</i>	<i>n</i>	<i>S</i>	ρ	$\langle d_i \rangle$	σ_{d_i}	d_{\max}
social (online)	facebook_0	0.43	0.03	0.37	324	0.97	0.05	15.52	1.00	77
	facebook_107	0.50	0.04	0.47	1034	1.00	0.05	51.74	0.91	253
	facebook_348	0.49	0.04	0.45	224	1.00	0.13	28.50	0.78	99
	facebook_414	0.65	0.03	0.62	148	0.99	0.16	22.86	0.56	57
	facebook_686	0.45	0.03	0.40	168	1.00	0.12	19.71	0.81	77
	facebook_698	0.66	0.01	0.59	40	0.66	0.28	11.00	0.52	29
	facebook_1684	0.45	0.04	0.41	775	0.99	0.05	36.14	0.79	136
	facebook_1912	0.70	0.02	0.70	744	1.00	0.11	80.71	0.80	293
	facebook_3437	0.45	0.03	0.37	532	1.00	0.03	18.09	0.81	107
	facebook_3980	0.44	0.04	0.35	44	0.85	0.15	6.27	0.66	18
	facebook_combined	0.52	0.02	0.55	4039	1.00	0.01	43.69	1.20	1045
Average		0.52	0.03	0.48	733.82	0.95	0.10	30.39	0.80	199.18

s - global similarity (clustering)

c - global complementarity

h - global complementarity (weak)

n - number of nodes in the giant component

S - relative size of the giant component

ρ - edge density

$\langle d_i \rangle$ - average node degree

σ_{d_i} - coefficient of variation of node degrees

d_{\max} - maximum node degree

Table S5. Descriptive statistics for *C. elegans* interactomes ($N = 10$)

domain	network	<i>s</i>	<i>c</i>	<i>h</i>	<i>n</i>	<i>S</i>	ρ	$\langle d_i \rangle$	σ_{d_i}	d_{\max}
biological	BPmaps	0.02	0.04	0.05	345	0.64	0.01	2.32	1.29	28
	Genetic	0.19	0.02	0.14	683	0.90	0.01	4.52	1.18	56
	IntegratedNetwork	0.47	0.01	0.45	5966	0.97	0.01	59.39	2.11	1001
	Interolog	0.44	0.08	0.69	2378	0.87	0.00	11.08	1.91	270
	LCI	0.00	0.01	0.03	117	0.27	0.02	2.10	3.93	90
	Microarray	0.52	0.01	0.49	2333	0.96	0.05	117.32	1.44	931
	Phenotypes	0.35	0.02	0.25	889	0.97	0.06	50.96	0.93	351
	WI8	0.02	0.03	0.04	2214	0.88	0.00	3.20	1.87	99
	wi2004	0.02	0.04	0.05	1084	0.88	0.00	2.96	1.85	74
	wi2007	0.02	0.03	0.04	1108	0.74	0.00	2.71	1.85	84
Average		0.20	0.03	0.22	1711.70	0.81	0.02	25.66	1.84	298.40

s - global similarity (clustering)

c - global complementarity

h - global complementarity (weak)

n - number of nodes in the giant component

S - relative size of the giant component

ρ - edge density

$\langle d_i \rangle$ - average node degree

σ_{d_i} - coefficient of variation of node degrees

d_{\max} - maximum node degree

Table S6. Descriptive statistics for software dependency networks ($N = 17$)

domain	network	<i>s</i>	<i>c</i>	<i>h</i>	<i>n</i>	<i>S</i>	ρ	$\langle d_i \rangle$	σ_{d_i}	d_{\max}
technological	colt	0.12	0.10	0.25	504	0.92	0.01	4.52	1.94	87
	flamingo	0.18	0.08	0.21	228	0.59	0.02	4.31	1.07	39
	guava	0.15	0.03	0.23	457	0.55	0.01	4.05	1.69	62
	java	0.01	0.01	0.23	2378	1.00	0.01	12.30	6.25	2166
	javax	0.09	0.19	0.35	1570	0.47	0.01	9.16	2.19	298
	jdk	0.01	0.06	0.21	6434	0.99	0.00	16.68	7.61	5923
	jmail	0.19	0.06	0.23	192	0.68	0.03	5.08	1.25	48
	jung	0.14	0.07	0.16	398	0.75	0.01	4.74	1.40	88
	jung-c	0.13	0.10	0.23	879	0.85	0.01	4.66	1.70	88
	jung-j	0.01	0.06	0.22	6120	1.00	0.00	16.43	7.70	5655
	junit	0.21	0.12	0.34	105	0.58	0.05	5.56	1.18	41
	org	0.11	0.08	0.36	486	0.61	0.02	11.18	2.30	255
	scolt	0.12	0.10	0.25	504	0.92	0.01	4.52	1.94	87
	sjbullet	0.18	0.07	0.19	249	0.81	0.03	6.44	1.22	73
	sjung	0.14	0.07	0.16	399	0.75	0.01	4.74	1.40	88
	slucene	0.06	0.09	0.22	2811	0.81	0.00	7.64	2.61	423
	weka	0.03	0.10	0.22	1225	0.58	0.01	7.73	3.39	580
Average		0.11	0.08	0.24	1467.00	0.75	0.01	7.63	2.76	941.24

s - global similarity (clustering)

c - global complementarity

h - global complementarity (weak)

n - number of nodes in the giant component

S - relative size of the giant component

ρ - edge density

$\langle d_i \rangle$ - average node degree

σ_{d_i} - coefficient of variation of node degrees

d_{\max} - maximum node degree

Table S7. Descriptive statistics for other network datasets ($N = 4$)

domain	network	<i>s</i>	<i>c</i>	<i>h</i>	<i>n</i>	<i>S</i>	ρ	$\langle d_i \rangle$	σ_{d_i}	d_{\max}
biological	reactome	0.61	0.05	0.63	5973	0.94	0.01	48.81	1.39	855
informational	game_thrones	0.33	0.02	0.25	107	1.00	0.06	6.58	1.00	36
social (offline)	jazz_collab	0.52	0.02	0.42	198	1.00	0.14	27.70	0.63	100
technological	internet_as	0.01	0.00	0.03	22963	1.00	0.00	4.22	7.81	2390
Average		0.37	0.02	0.34	7310.25	0.99	0.05	21.83	2.71	845.25

s - global similarity (clustering)

c - global complementarity

h - global complementarity (weak)

n - number of nodes in the giant component

S - relative size of the giant component

ρ - edge density

$\langle d_i \rangle$ - average node degree

σ_{d_i} - coefficient of variation of node degrees

d_{\max} - maximum node degree

S5. Overfitting robustness of module detection based on structural coefficients

Here we present a preliminary analysis of the robustness of our naive method for detecting groups of structurally similar and/or complementary nodes used in Sec. 2.8. For this purpose we plotted modularity scores with respect to different significance level (α) thresholds in the observed unweighted/weighted co-appearances network as well as a randomized instance sampled from the corresponding null model (UBCM/UECM).

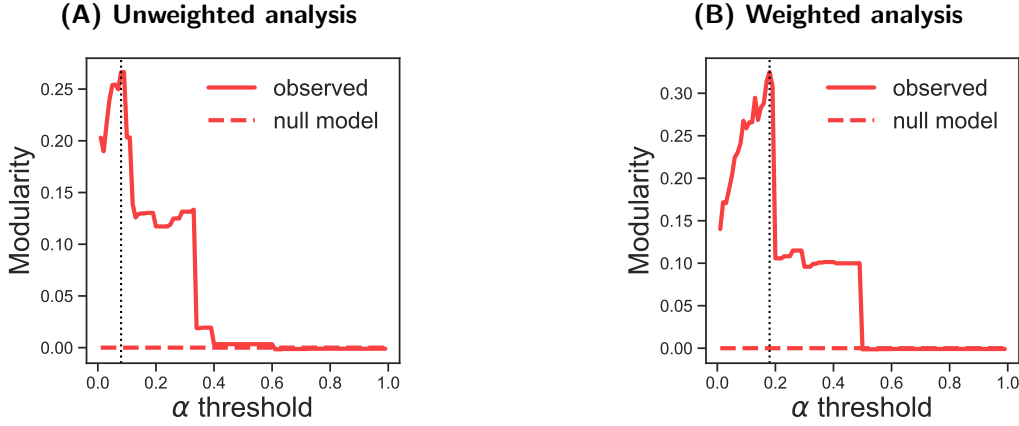


Figure S1. Modularity scores with respect to α thresholds when using the proposed method for detecting groups of structurally similar and/or complementary nodes.

Clearly in both cases the modularity curve with respect to α is first increasing towards the optimal point after which it suddenly starts to decrease quickly reaching near zero values. On the other hand, the modularity curves in the randomized networks are completely flat and stay at zero. In other words, the method does not detect any groups in the randomized networks indicating that the method does not overfit and detect clusters in purely random networks (at least in this particular case).

S6. Groups of structurally similar characters with all labels

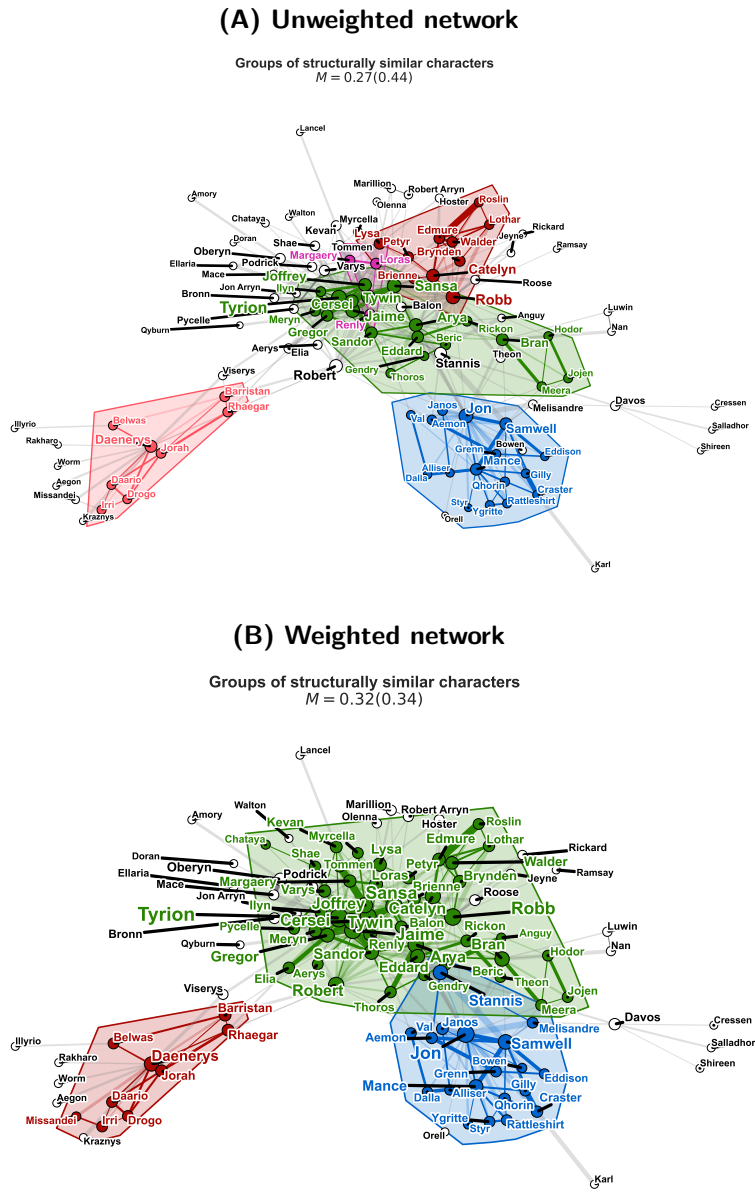


Figure S2. Groups of structurally similar characters with labels in the network of co-appearances in A Storm of Swords.